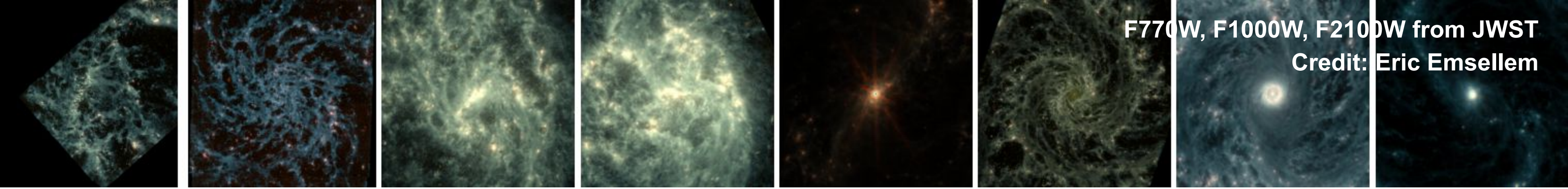

Structure and porosity of the multiphase ISM in nearby spatially resolved galaxies

Lise Ramambason, Postdoc at the University of Heidelberg
Institut für Theoretische Astrophysik

Emmy Noether-Programm
DFG Deutsche Forschungsgemeinschaft

18th Potsdam Thinkshop: The role of feedback in galaxy formation, from small scale winds to large scale outflows - 14/07/25

UNIVERSITÄT HEIDELBERG ZUKUNFT SEIT 1386

ZENTRUM FÜR ASTRONOMIE

Phangs

I - Context : ISM structure, porosity, and time-evolution

How does the porosity of ionizing photons impact the multi-scale ISM ?

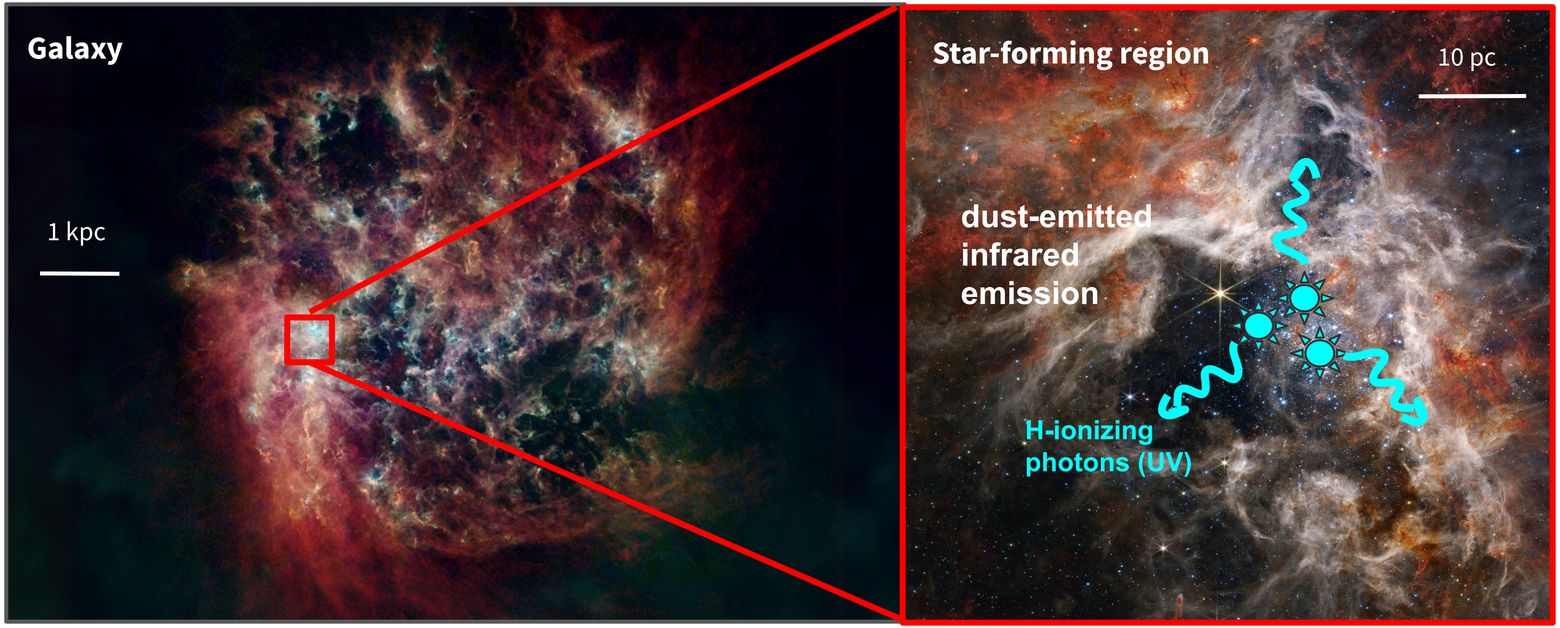

Large **diffuse ionized gaz** reservoirs (20-60%)
Della Bruna+21, Belfiore+22

Escape fractions $< f_{esc,\,HII} >$ **~ 0 - 70 %**
Pellegrini+12, Choi+20, Della Bruna+21, Barnes+22
Ramambason+22, Teh+23, Scheuermann+in prep

The ISM structure and porosity vary **with spatial scales… and time !**

I - Context : ISM structure, porosity, and time-evolution

Constraining the evolutionary timeline of gas, dust, and stars in SF regions

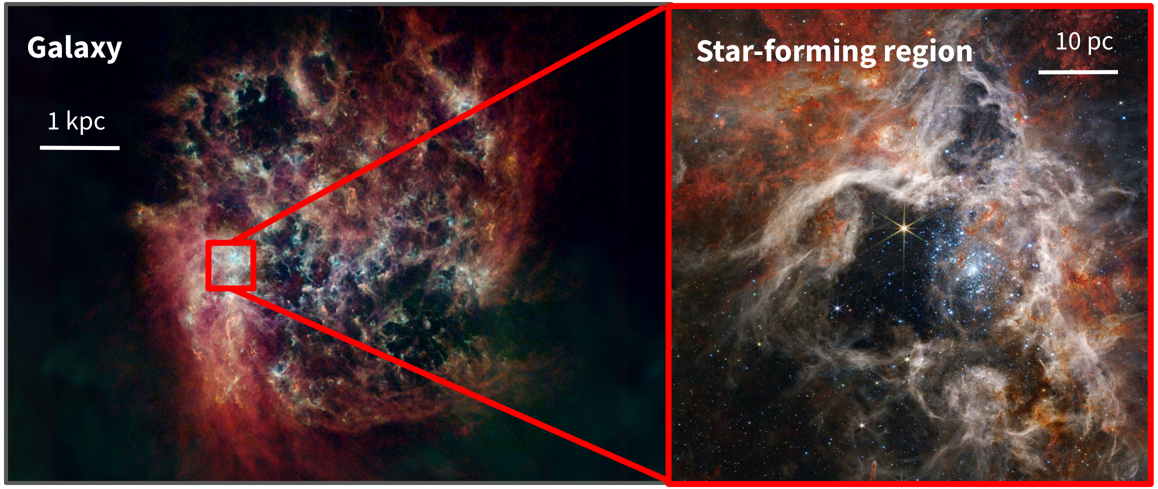

Theoretical approaches :
- GMC-scale simulations
e.g., STARFORGE Grudić et al. 2018
- Semi-analytic 1D models
e.g., WARPFIELD, Pellegrini+20

See Jia Wei Teh's poster on TRINITY feedback model !

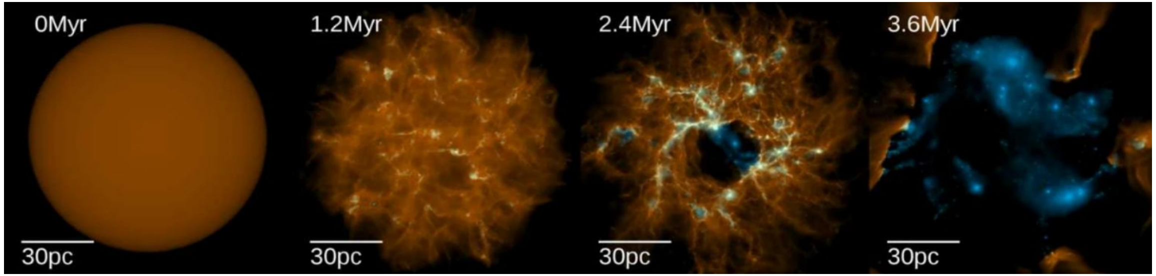

Constraints from observations :
- dynamics of expanding regions
- cluster age
- **spatial distribution of the gas vs. SFR around peaks**

Large Magellanic Cloud, ESA/NASA/JPL-Caltech/CSIRO/C. Clark (STScI), Fahrion et al. 2024, STARFORGE Grudić et al. 2018

I - Context : ISM structure, porosity, and time-evolution

Constraining the evolutionary timeline of gas, dust, and stars in SF regions

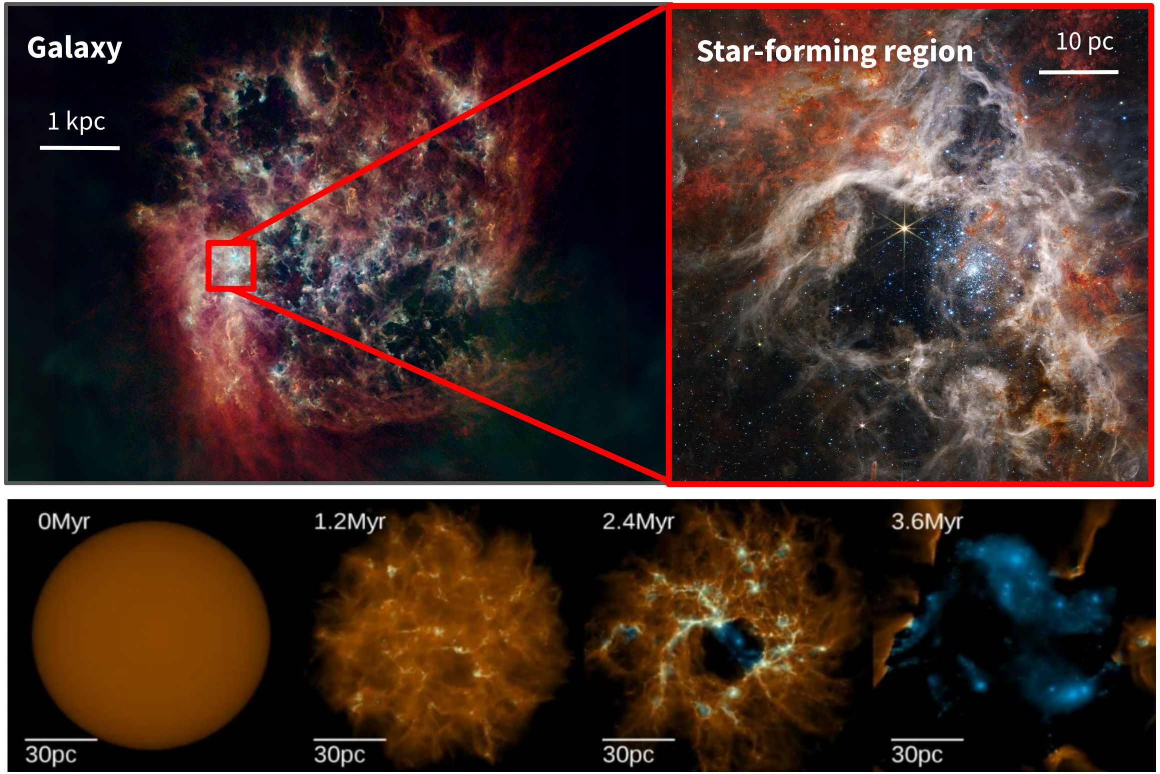

- **How long do stars stay embedded in dust and gas** before they
  1. emerge in the optical,
  2. destroy their host cloud ?

- Which **physical processes are driving these transitions, and are they universal** ?

Large Magellanic Cloud, ESA/NASA/JPL-Caltech/CSIRO/C. Clark (STScI), Fahrion et al. 2024, STARFORGE Grudić et al. 2018

II - Data: PHANGS-JWST surveys, mid-IR imaging of 74 nearby galaxies

Lee et al. 2023, Williams et al. 2024, Chown et al. 2025 (Cycle 1, PI: J. Lee + Cycle 2, PI A. Leroy)

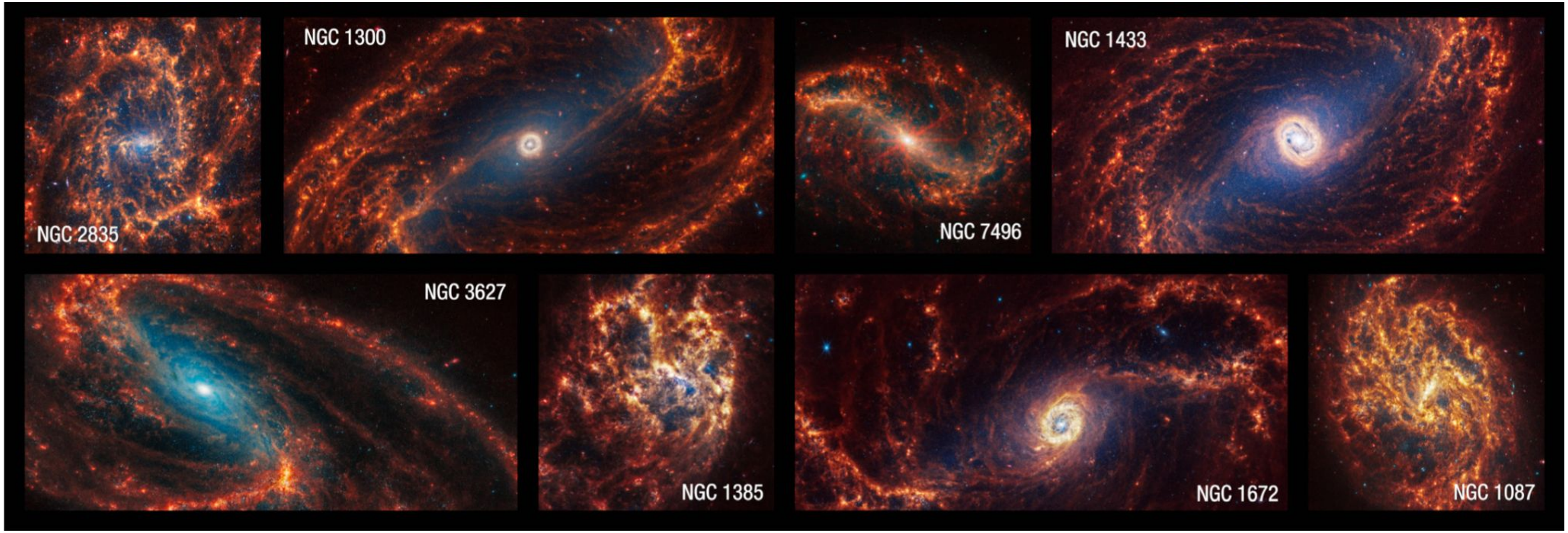

Williams et al. 2024

8 MIRI + NIRCam bands :

PAH tracing bands

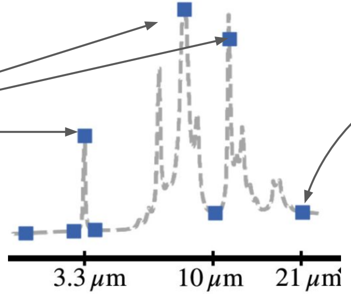

continuum-dominated band at **21μm** ⇒ proxy for embedded SFR

Belfiore et al. 2023

See Oleg Egorov's talk on Tuesday !

II - Constraining the duration and properties of the embedded SF phase in the PHANGS-JWST survey (Ramambason+subm, arXiv:2507.01508)

PHANGS-ALMA : Leroy et al. (2021)
PHANGS-Hα: Razza et al. subm
PHANGS-MUSE: Emsellem et al. (2022)
PHANGS-JWST: Lee et al. (2023), Williams et al. (2024), Chown et al. (2025)

See also Debosmita Pathak's poster on HII region's feedback

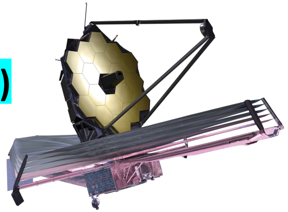

ALMA/CO(2-1) | **early "embedded" star formation** | **Hα**

STARFORGE
Grudić et al. 2018

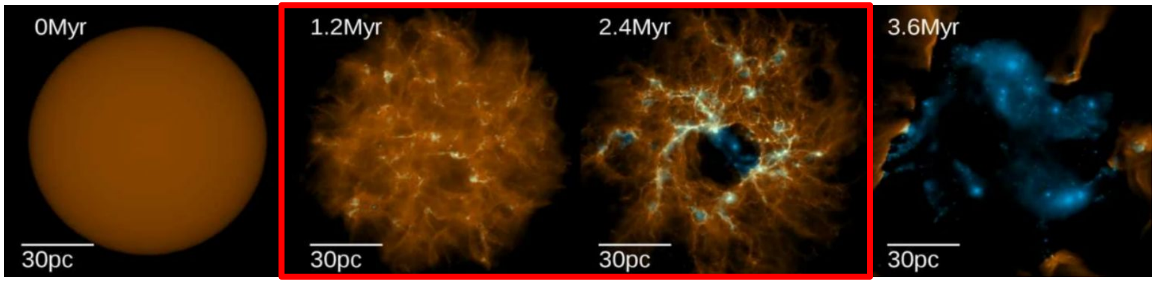

Sub-sample selection : - observed in CO, 21μm, and Hα
- sufficient resolution (< 180pc) to resolve decorrelation between 21μm and CO
⇒ 37 galaxies with a wide range of physical properties and morphologies

III . Method : interpreting gas and stars de-corellations with the "tuning-fork"

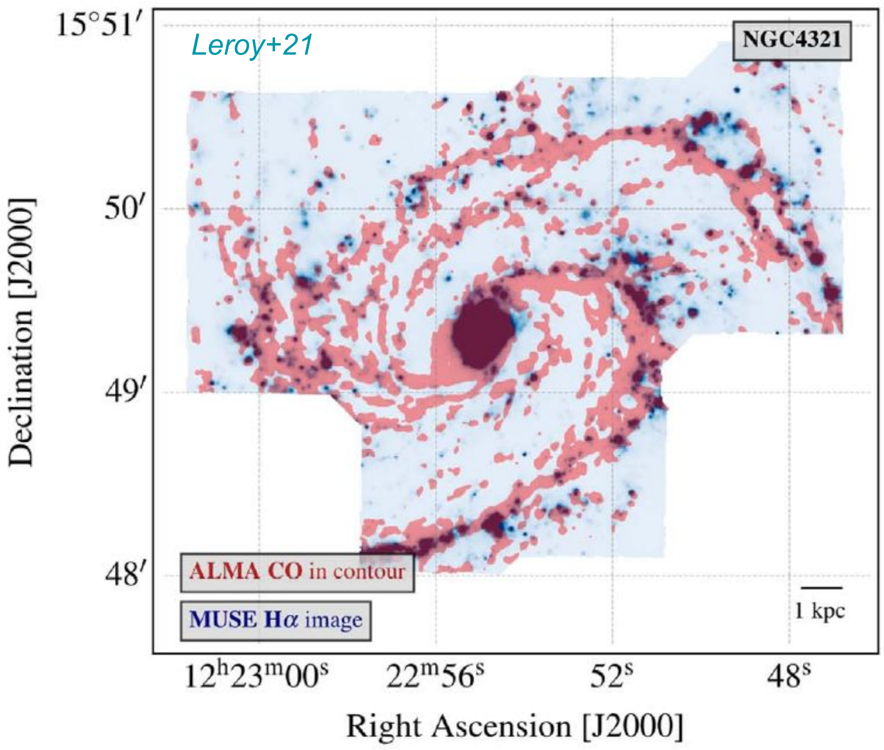

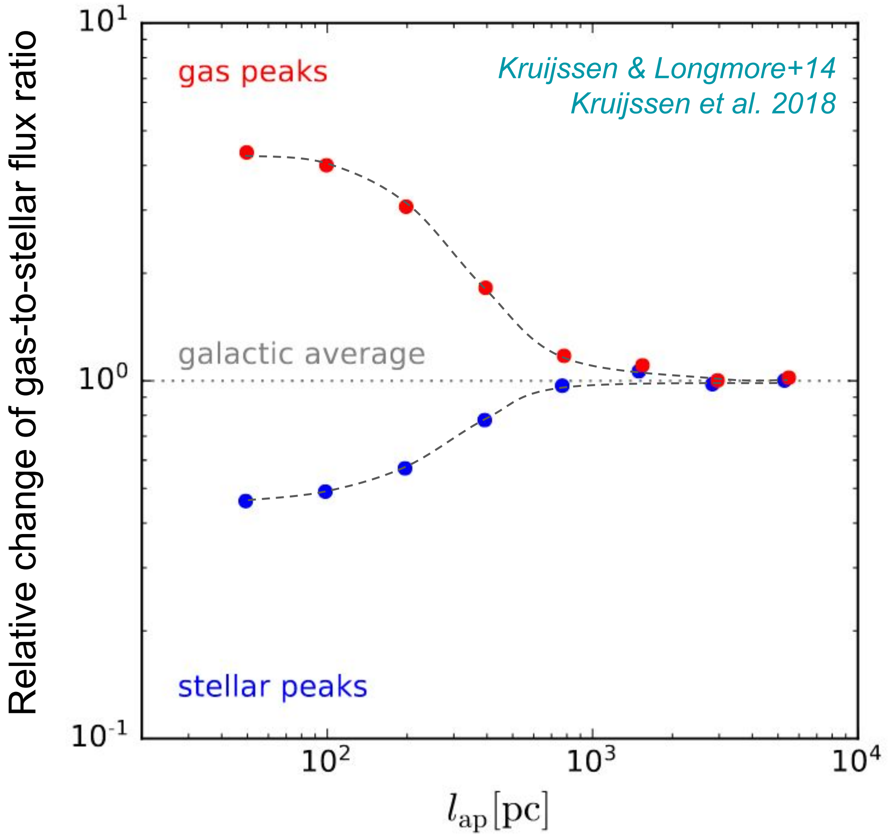

Main assumption : the observed clouds population samples the GMCs evolutionary timeline

III . Method : interpreting gas and stars de-corellations with the "tuning-fork"

$$\mathcal{B}_{\rm gas}^{\rm mod} = \frac{f_{\rm gas} + \frac{t_{\rm gas}}{\tau}\left(\frac{l_{\rm ap}}{\lambda}\right)^2}{f_{\rm star}\left[1+\beta_{\rm star}^{-1}\left(\frac{t_{\rm star}}{t_{\rm over}}-1\right)\right]^{-1} + \frac{t_{\rm gas}}{\tau}\left(\frac{l_{\rm ap}}{\lambda}\right)^2},$$

$$\mathcal{B}_{\rm star}^{\rm mod} = \frac{f_{\rm gas}\left[1+\beta_{\rm gas}^{-1}\left(\frac{t_{\rm gas}}{t_{\rm over}}-1\right)\right]^{-1} + \frac{t_{\rm star}}{\tau}\left(\frac{l_{\rm ap}}{\lambda}\right)^2}{f_{\rm star} + \frac{t_{\rm star}}{\tau}\left(\frac{l_{\rm ap}}{\lambda}\right)^2},$$

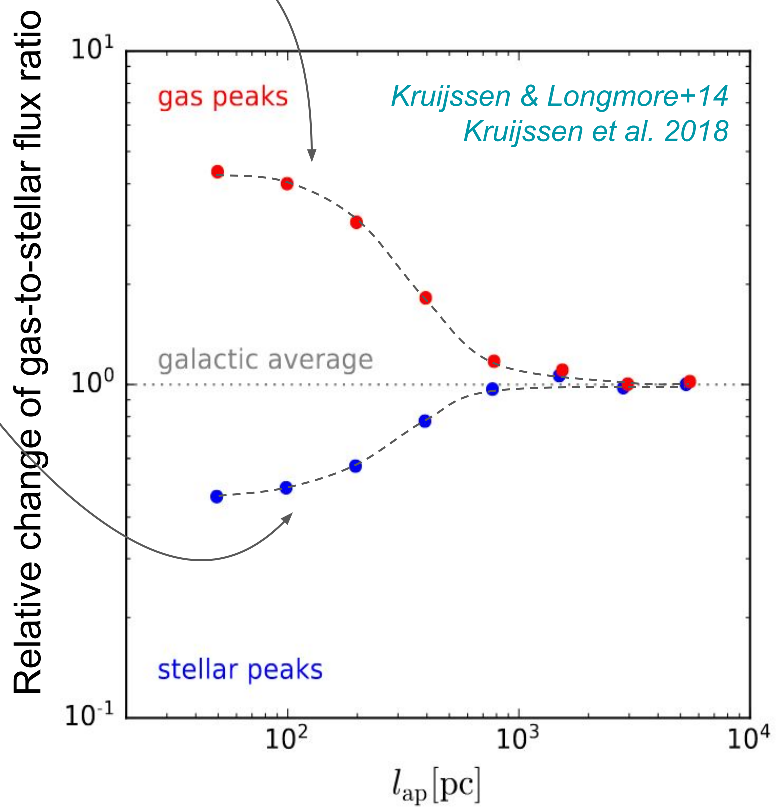

3 independent parameters:

- **t_{gas}** : the timescale of emission of the gas tracer
- **t_{over}**: the timescale of feedback
- **λ**: the spatial scale at which the SFR and gas tracers decorrelate

IV. Results : measuring the timescales associated with the dust-embedded SF

PHANGS-ALMA : Leroy et al. (2021)
PHANGS-Hα: Razza et al. subm
PHANGS-JWST: Lee et al. (2023),
Williams et al. (2024), Chown et al. (2025)

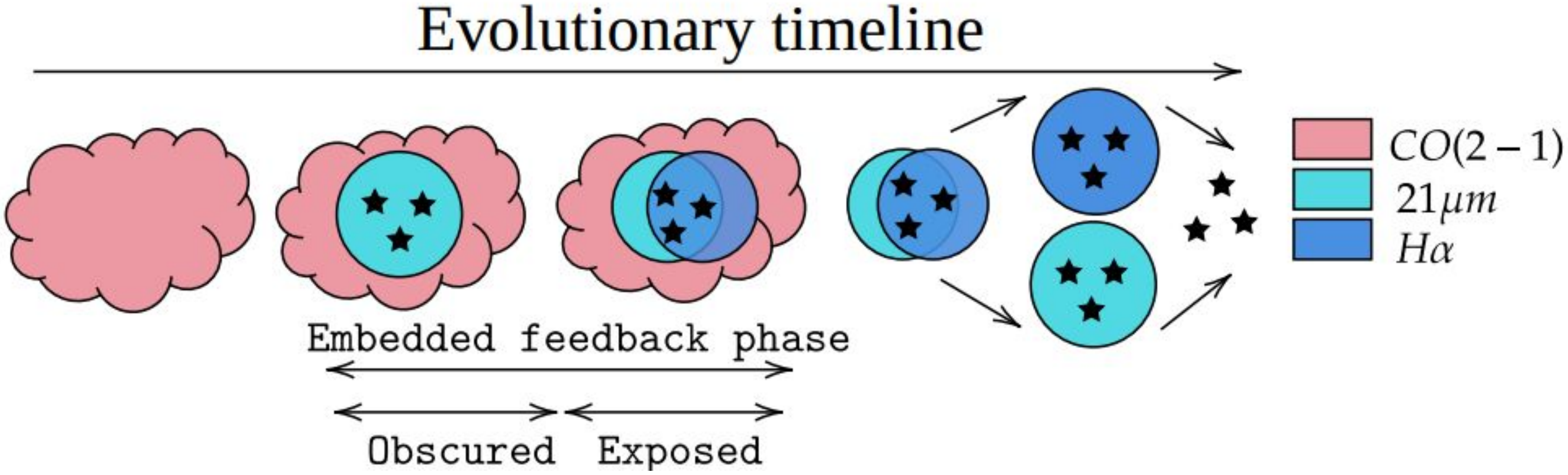

IV. Results : measuring the timescales associated with the dust-embedded SF

PHANGS-ALMA : Leroy et al. (2021)
PHANGS-Hα: Razza et al. subm
PHANGS-JWST: Lee et al. (2023),
Williams et al. (2024), Chown et al. (2025)

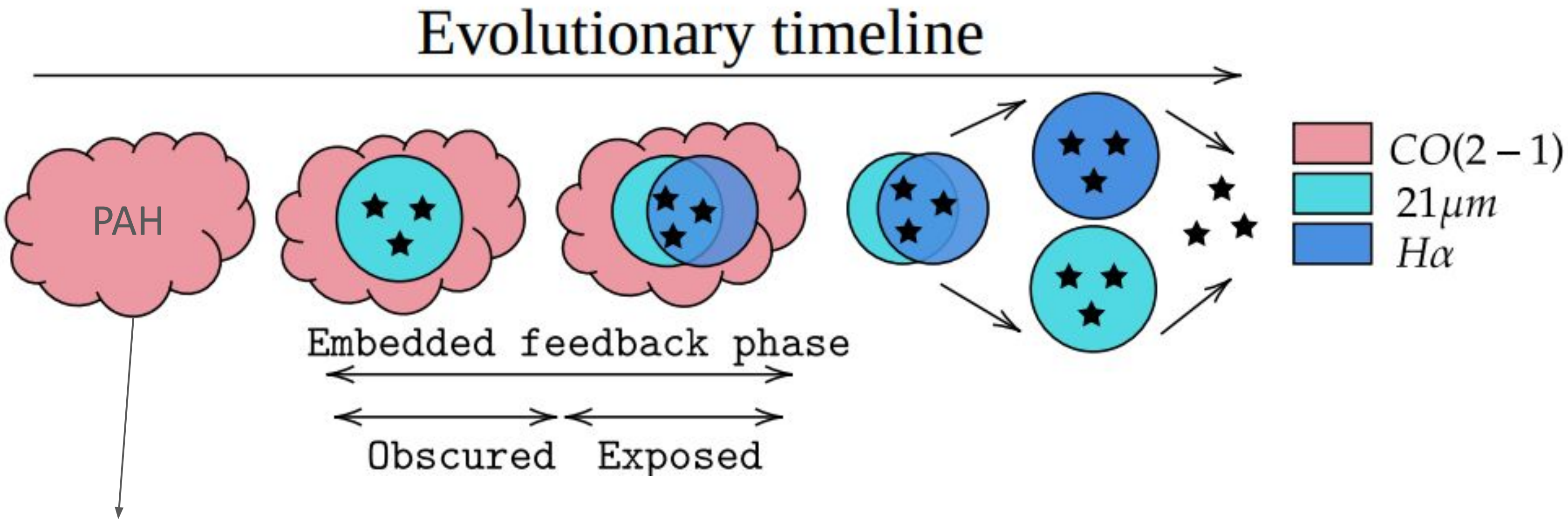

Timescales associated with PAH emission (Kim, Chevance, Ramambason et al. 2025)

IV. Results : measuring the timescales associated with the dust-embedded SF

1. Is the dust-obscured phase of star-formation short in all galaxies ?

Ramambason et al. subm

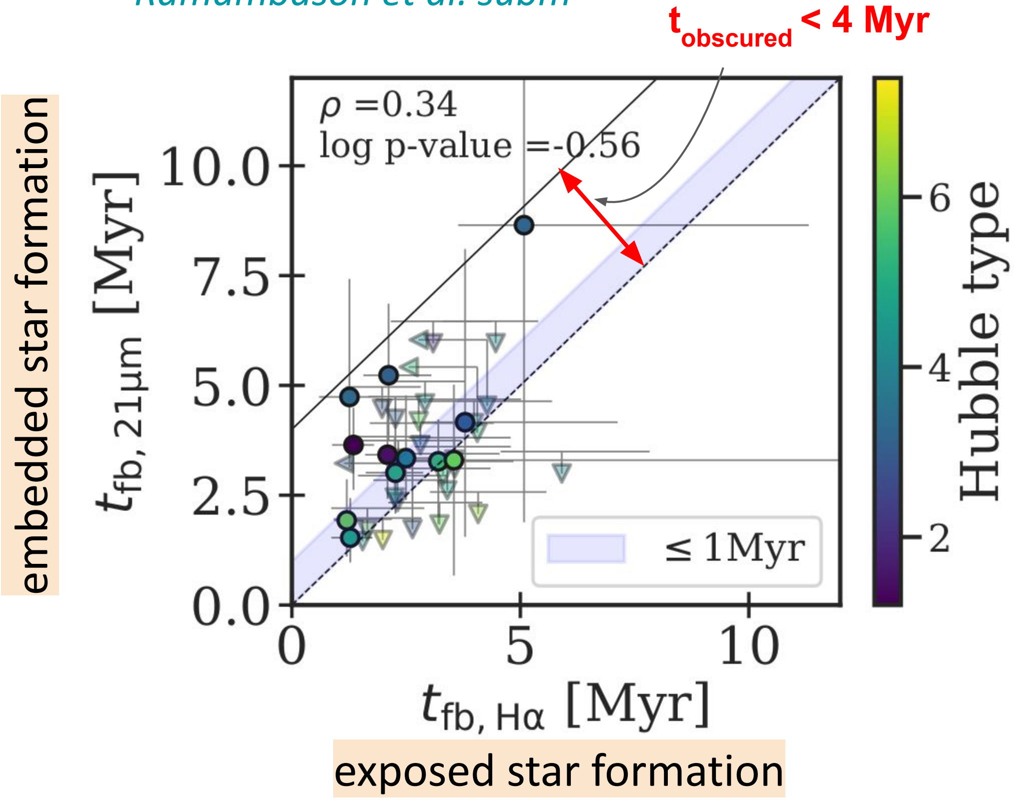

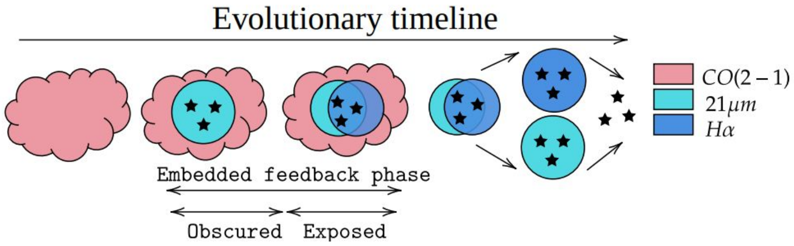

- The **embedded star-formation phase is short (<4 Myr)** in all the galaxies
- **< 1 Myr** for 28/37 galaxies.

IV. Results : measuring the timescales associated with the dust-embedded SF

1. Is the dust-obscured phase of star-formation short in all galaxies ?

Ramambason et al. subm

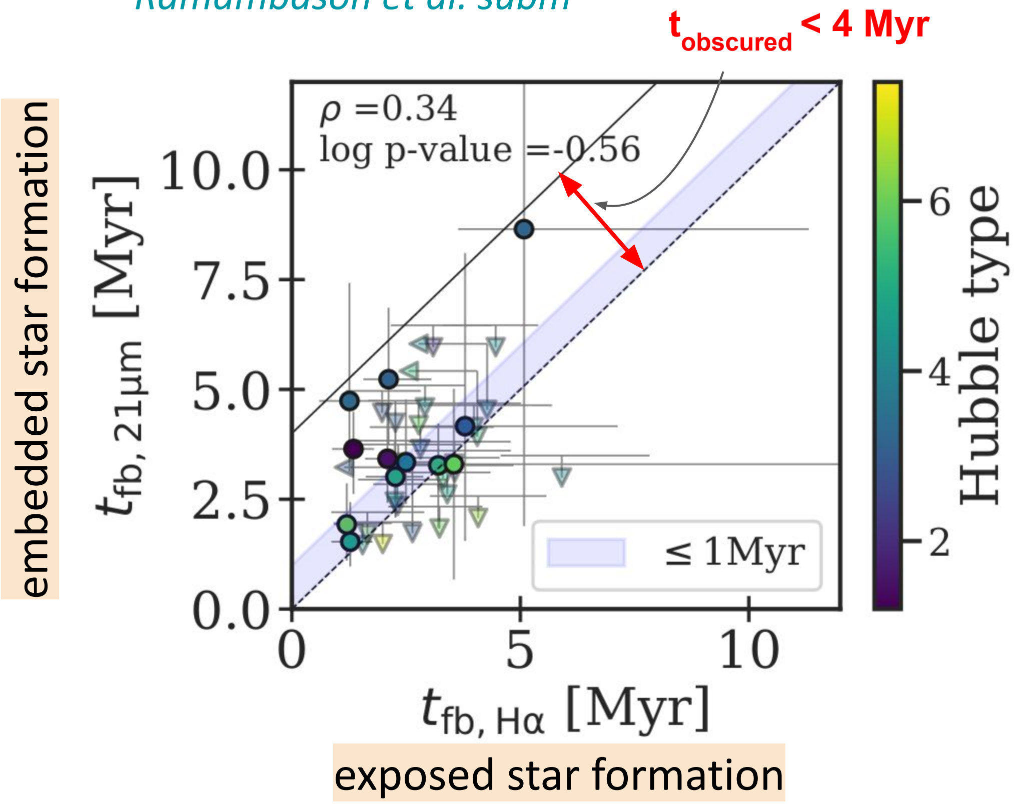

⇒ Feedback timescales consistent with **pre-supernova feedback (< 4 - 5Myr)** *e.g, Chevance+20,+22, Kim+21,+23*

⇒ $t_{obscured}$ consistent with age estimates of **dust-embedded young stellar populations ~ 1 - 4 Myr** *e.g, Whitmore+15, Hollyhead+15, Grasha+18, Deshmuk+24, Sun+24, Rodriguez+25, Whitmore+25*

- longer dust-obscured star-formation phase **barred spiral galaxies**

IV. Results : measuring the timescales associated with the dust-embedded SF

2. Which parameters regulate the timescales of the dust emission at 21um ?

Ramambason et al. subm

Total duration of 21µm emission

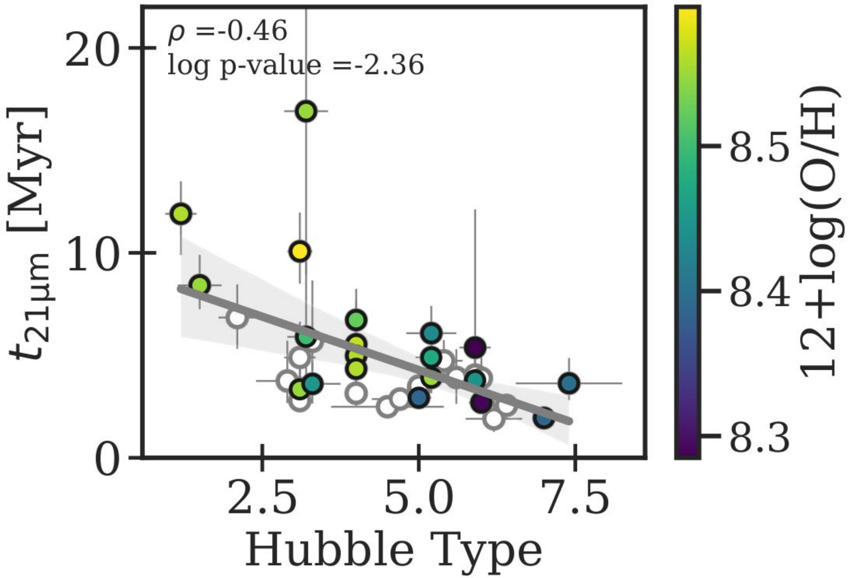

Duration of the obscured SF phase

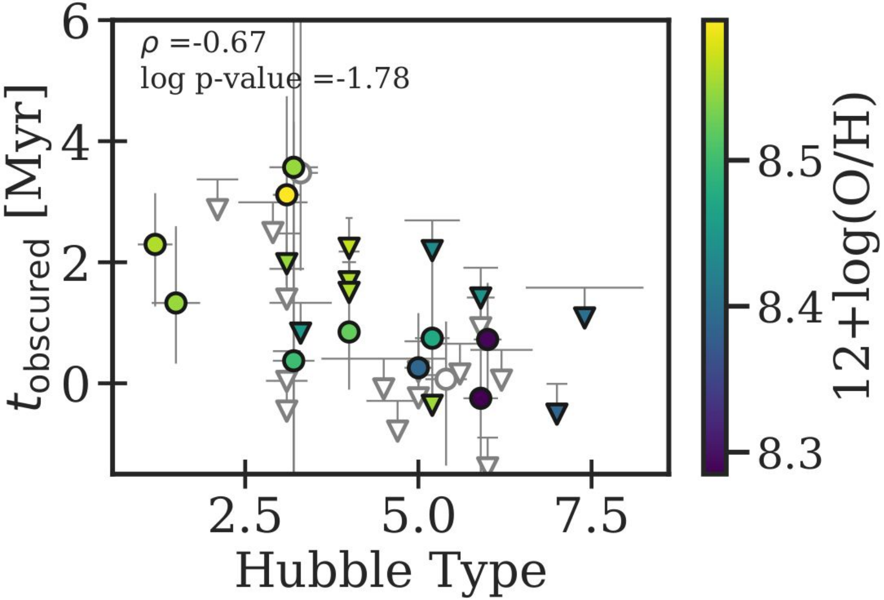

⇒ **Reduced duration** of the 21µm emission and obscured star-formation phase:

- later type galaxies (**flocculent and irregular morphologies**)
- lower **metallicities** (from PHANGS-MUSE, *Emsellem+22, Williams+22*)

IV. Results : measuring the timescales associated with the dust-embedded SF

2. Which parameters regulate the timescales of the dust emission at 21um ?

Ramambason et al. subm

Total duration of 21µm emission

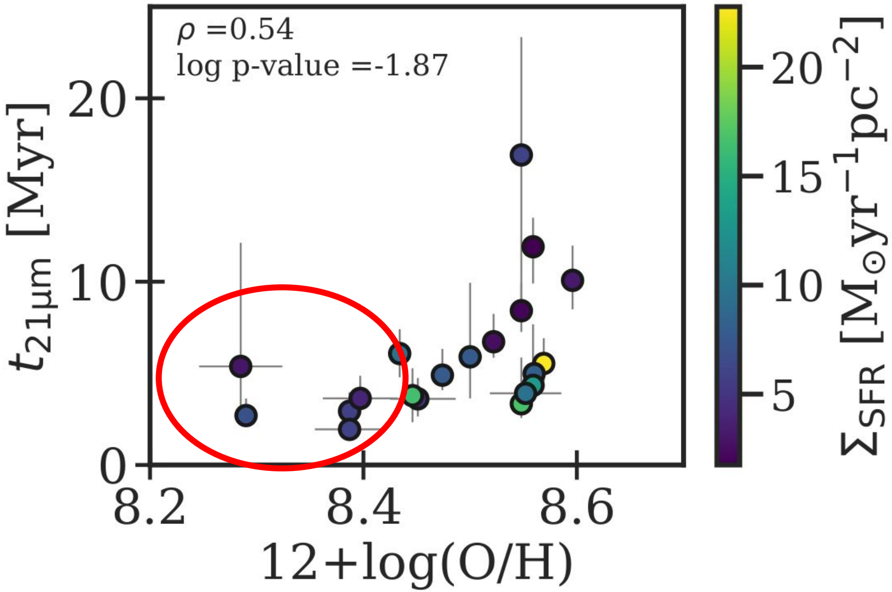

Duration of the obscured SF phase

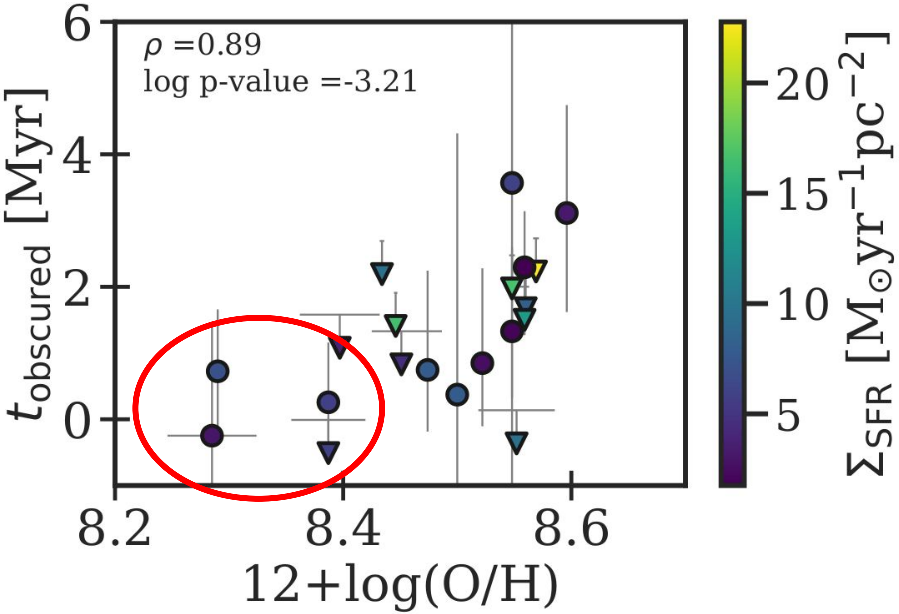

⇒ reduced duration of the 21µm emission and duration obscured SF phase in galaxies with <u>lower metallicity ?</u> → **effect of increased ISM porosity at low-metallicity ?**

Observed at galactic scales e.g., Cormier+19, Chevance+20b, Ramambason+22,+24

V - Multicomponent modelling of low-metallicity HII regions (in prep)

Data : 6 dwarf galaxies observed with MUSE+HST (LEGUS-dwarf, Egorov+in prep)

Catalog with ~ 1700 nebular regions
~1100 HII regions (BPT classification)

Method : multicomponent modelling with MULTIGRIS (Lebouteiller & Ramambason+22)

Combination of Cloudy models from a large grid of models, tailored for low-Z conditions
SFGX model grid, Ramambason+22

Cloudy models with single burst stellar cluster (metallicity, age)

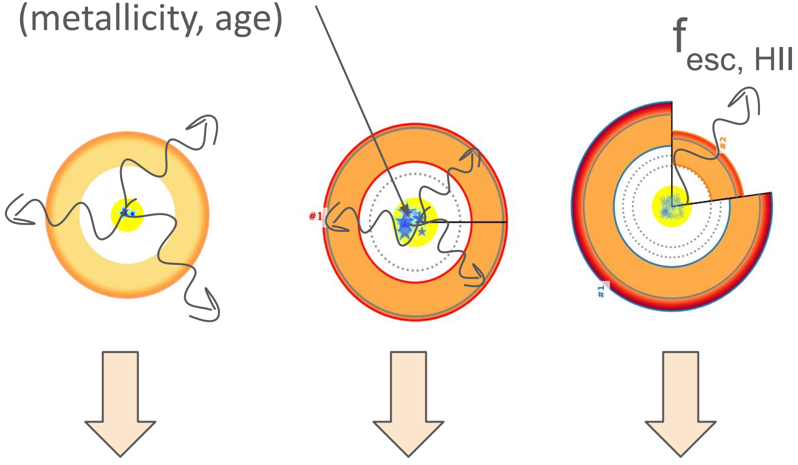

density-bounded HII region (n1, U1, fesc1)	radiation-bounded HII region (n1, U1, fesc1 = 0)	mix of 2 components $\left\{ \begin{array}{c} \text{n1, U1, fesc1} \\ \text{n2, U2, fesc2 = 0} \end{array} \right\}$

V - **MULTIGRIS**: a Bayesian tool for multicomponent ISM modelling

Lebouteiller & Ramambason 2022, GitLab: https://gitlab.com/multigris/mgris

SCAN ME

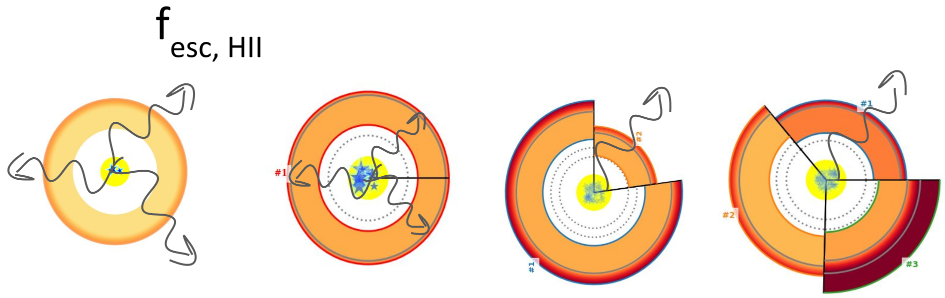

See Xinyue Liang's talk on Tuesday using <u>continuous distributions</u> of components (power-laws)

Increasing number of ISM components

also used in Ramambason+24, Varese+25, Lebouteiller+25, Richardson+in prep, Levanti+in prep

V - Multicomponent modelling of low-metallicity HII regions (in prep)

Output : predicted PDF of key parameters incl. the escape fraction from ~1100 HII regions

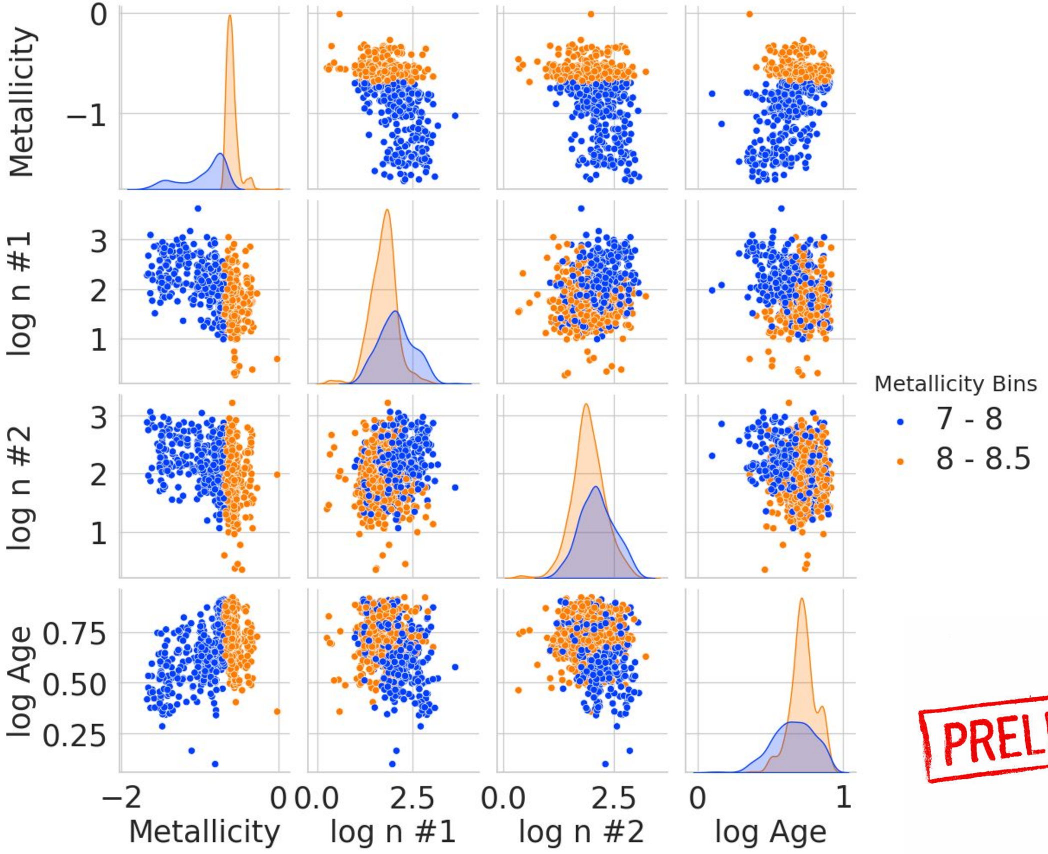

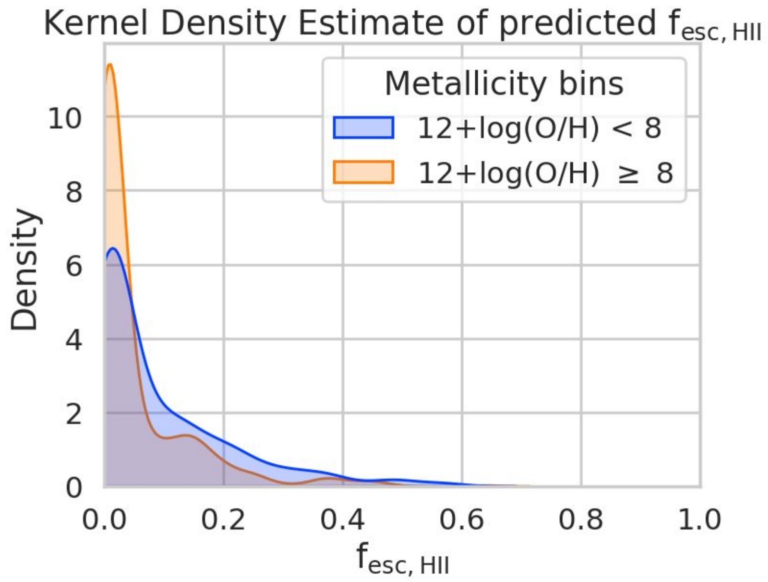

Higher predicted $f_{esc,HII}$ among lower metallicity HII regions ?

Main take-away

Ramambason+ subm (arXiv: 2507.01508)

- **The dust-obscured star-formation phase is typically short (< 1 Myr)**
- Feedback timescales hint at a predominant role from **pre-SN stellar feedback** **(< 4 - 5 Myr)**
- The 21μm timescales and timescale of embedded SF phase vary with:
  - morphological type
  - metal and dust content

… and future explorations !

⇒ Connecting GMC evolution with **the properties of HII regions / star clusters**

⇒ explore properties of **low-metallicity ISM and its porosity to ionizing photons ($f_{esc,HII}$)**

⇒ combine/compare **key quantities & timescales** derived with different approaches (e.g., statistical, modelling, simulation)

Back-up slides

I - Context : star formation and its dust-embedded phase

How to disentangle the signatures of stellar feedback mechanisms ?

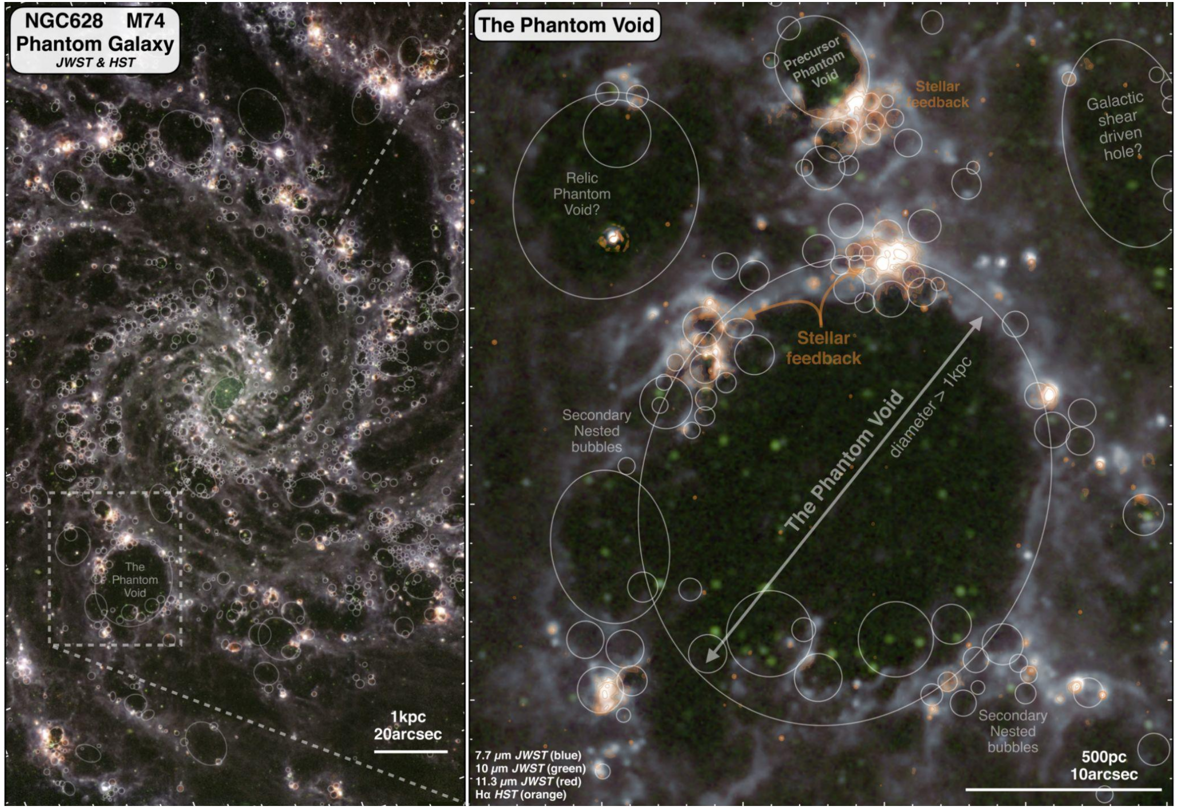

Barnes et al. 2023

Star formation cycle :

1. <u>how</u> it started ?
2. <u>how</u> efficient ?
3. <u>which</u> feedback processes ?

⇒ evolution over cosmic times

Multiscale, multiwavelength, and evolving processes

In this talk:

- *50 pc → 10 kpc*
- *mm → optical tracers*
- *GMC formation → destruction*

(10-30 Myr, Chevance et al. 2020, Kim et. al. 2022)

I - Context : star formation and its dust-embedded phase

The JWST reveals fainter and more compact sites of star formation

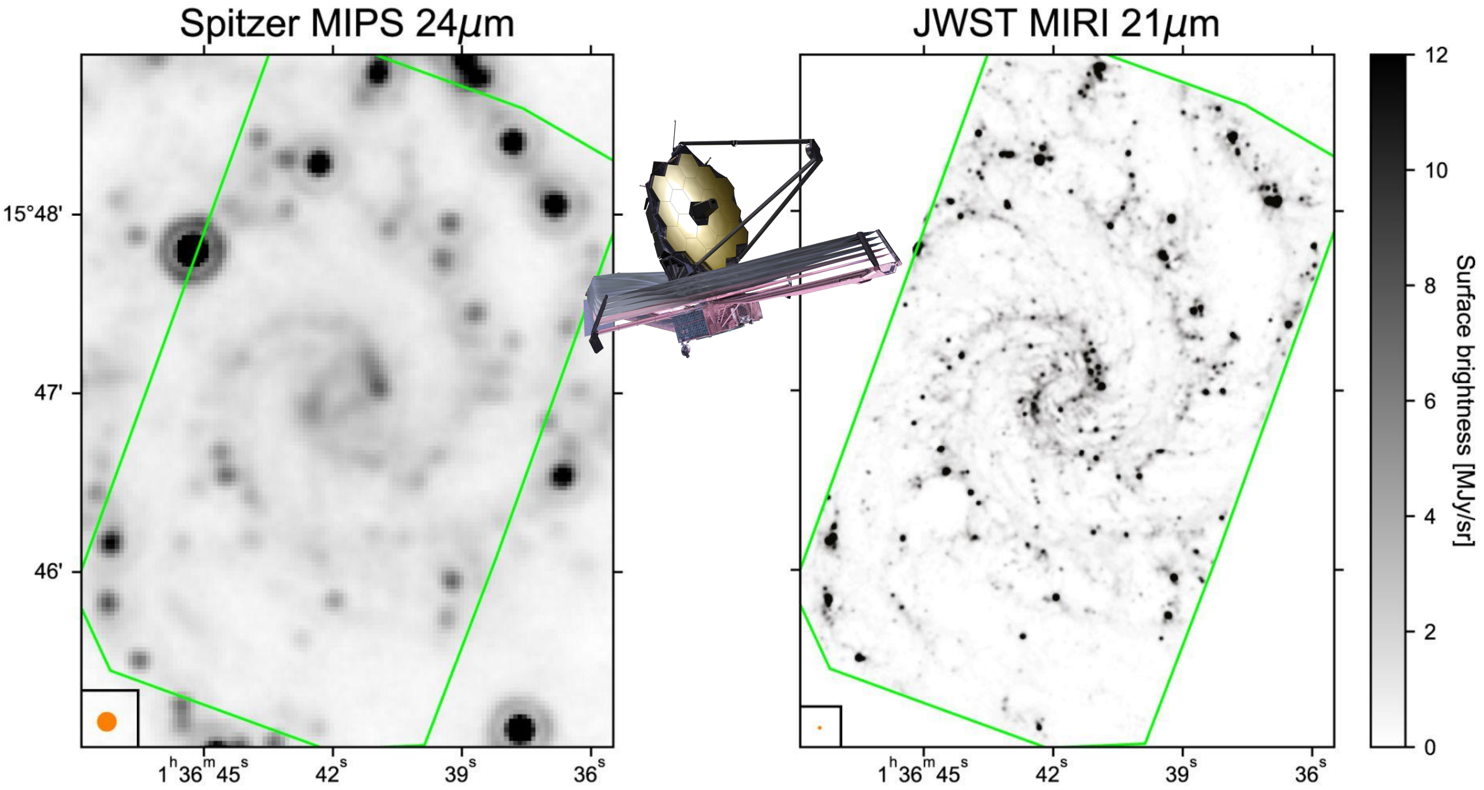

Galaxie NGC 628, Kim et al. 2023

- sensitivity
- spectral resolution
- spatial resolution

I - Context : ISM structure, porosity, and time-evolution

Constraining the evolutionary timeline of gas, dust, and stars in SF regions

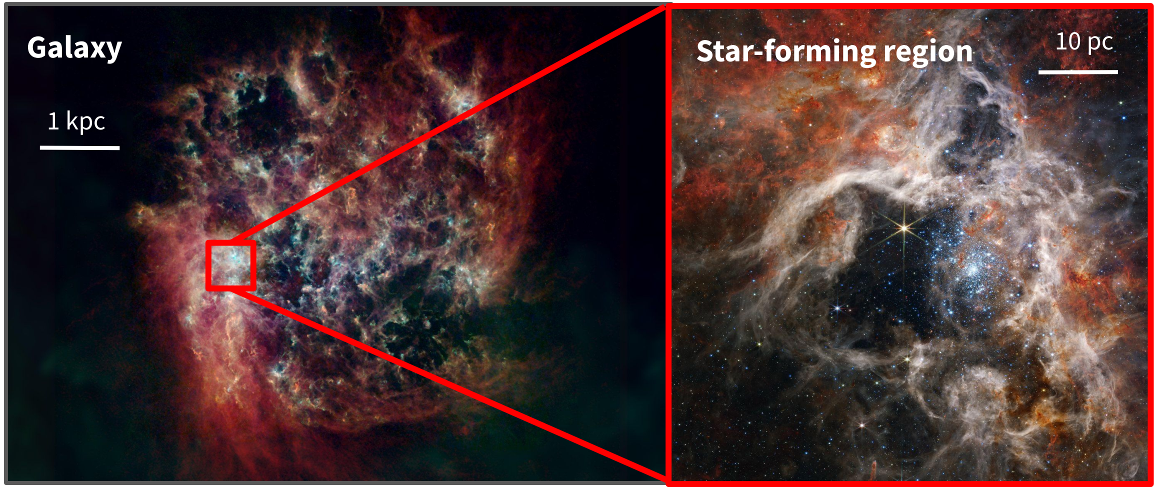

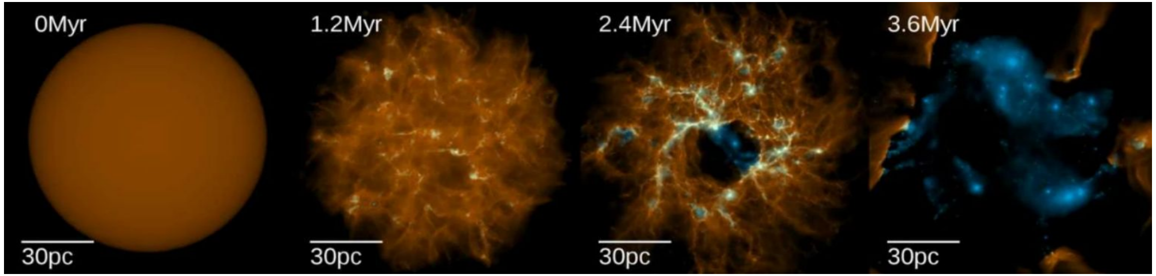

Large Magellanic Cloud, ESA/NASA/JPL-Caltech/CSIRO/C. Clark (STScI), Fahrion et al. 2024, STARFORGE Grudić et al. 2018

Evolutionary timelines of GMCs depend on :

→ **feedback mechanisms**
e.g., Smith+21, Semenov+21

→**GMC properties (incl. chemistry)**
e.g., Fukushima+20, Yoo+20

→ **galactic properties**
e.g., Chevance+20, Kim+22

… varies **within galaxies from region to region**
e.g., Chevance+22, Romanelli+25

II - Constraining the duration and properties of the embedded SF phase in the PHANGS-JWST survey (Ramambason+subm, arXiv:2507.01508)

Sub-sample selection : - observed in CO, 21μm, and Hα
- sufficient resolution (< 180pc) to resolve decorrelation between 21μm and CO
⇒ 37 galaxies with a wide range of physical properties and morphologies

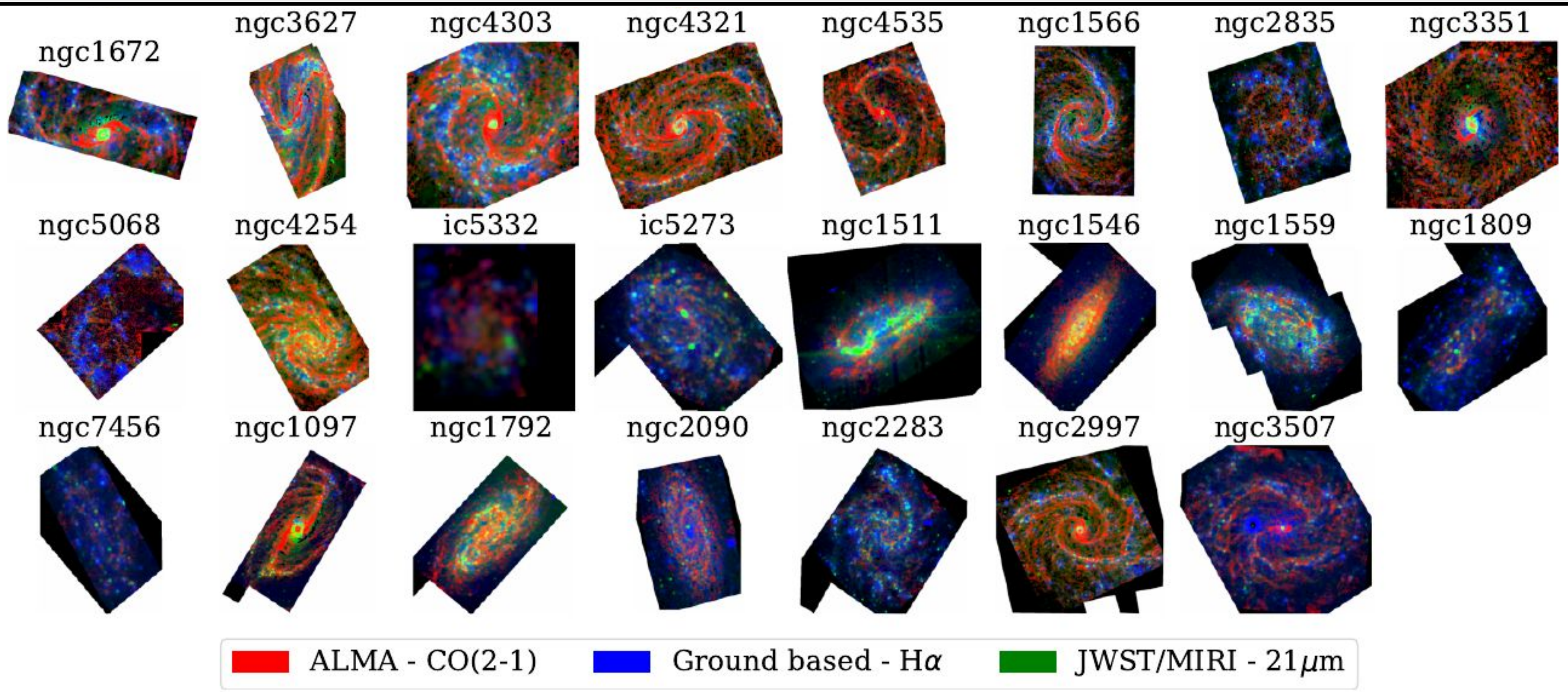

III . Method : interpreting gas and stars de-corellations with the "tuning-fork"

Kruijssen & Longmore 2014, Kruijssen et al. 2018

Kim et al. 2022

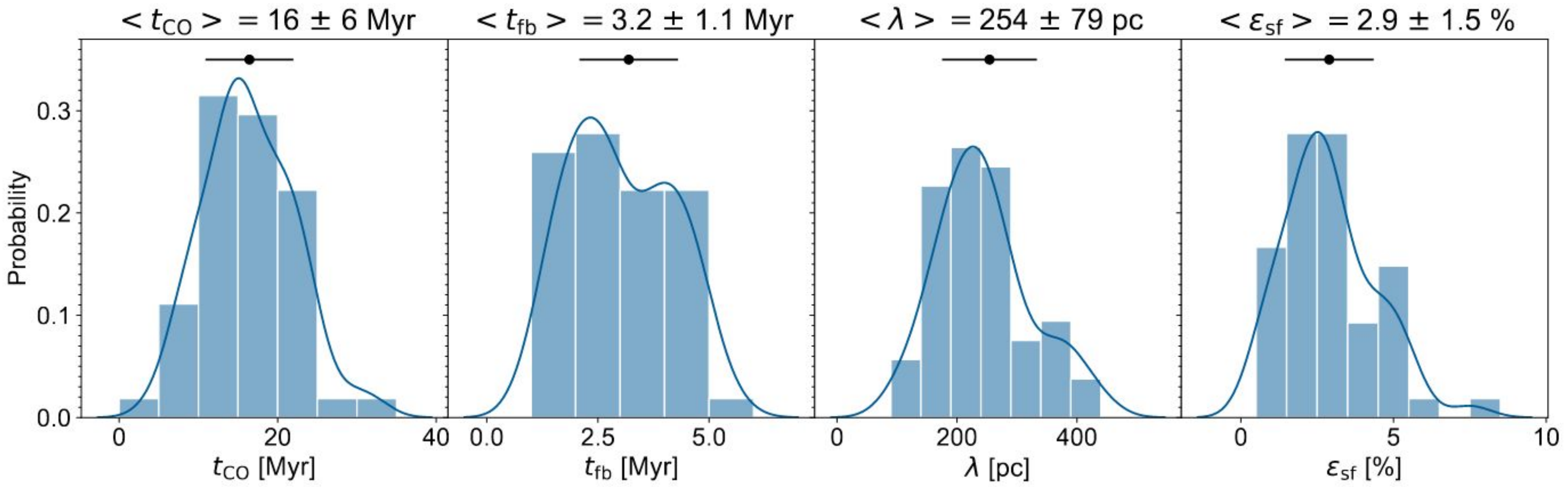

⇒ extensively applied to **local star forming galaxies**

e.g., Chevance et al. 2020a,b, 2022; Zabel et al. 2020; Kim et al. 2021, 2022, 2023; Ward et al. 2020, 2022; Lu et al. 2022; Kruijssen et al. 2024; Romanelli et al. 2025; Kim et al. 2025

and to **simulations**

e.g., Haydon et al. 2020; Fujimoto et al. 2019; Semenov et al. 2021; Keller et al. 2022

II - 2.Method : measuring the duration of the dust-obscured phase of SF

Kim et al. 2021, Kim et al. 2023

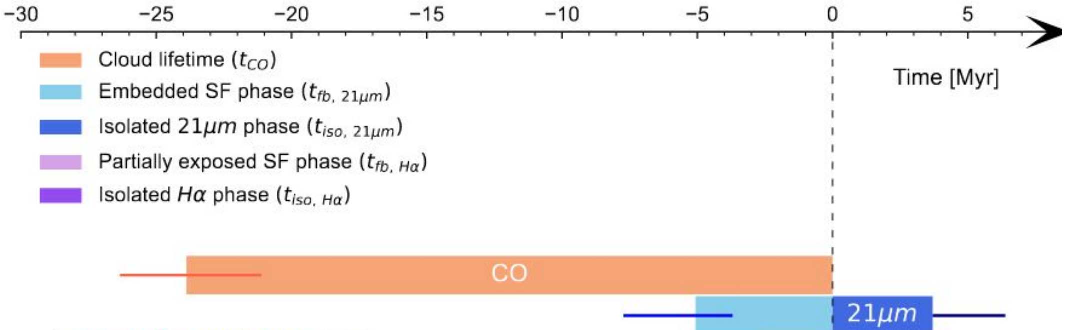

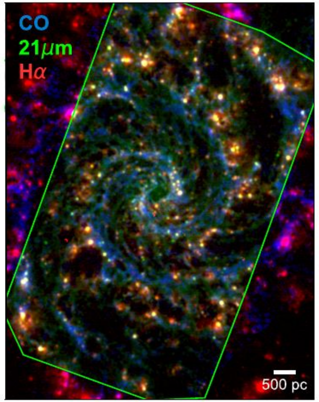

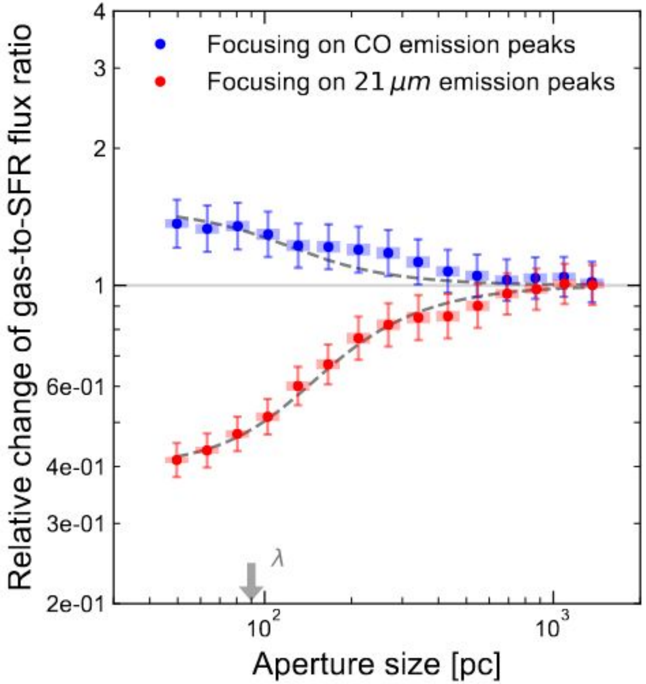

$\boxed{t_{obscured}(21\mu m) = \mathbf{2.3 \pm^{2.7}_{-1.4}\ Myr}}$

Is the dust-obscured phase of SF this short in all galaxies ? dependencies ?

III- 2. The tuning-fork method: exploiting spatial correlations between stars and gas

Kruijssen & Longmore+14
Kruijssen et al. 2018

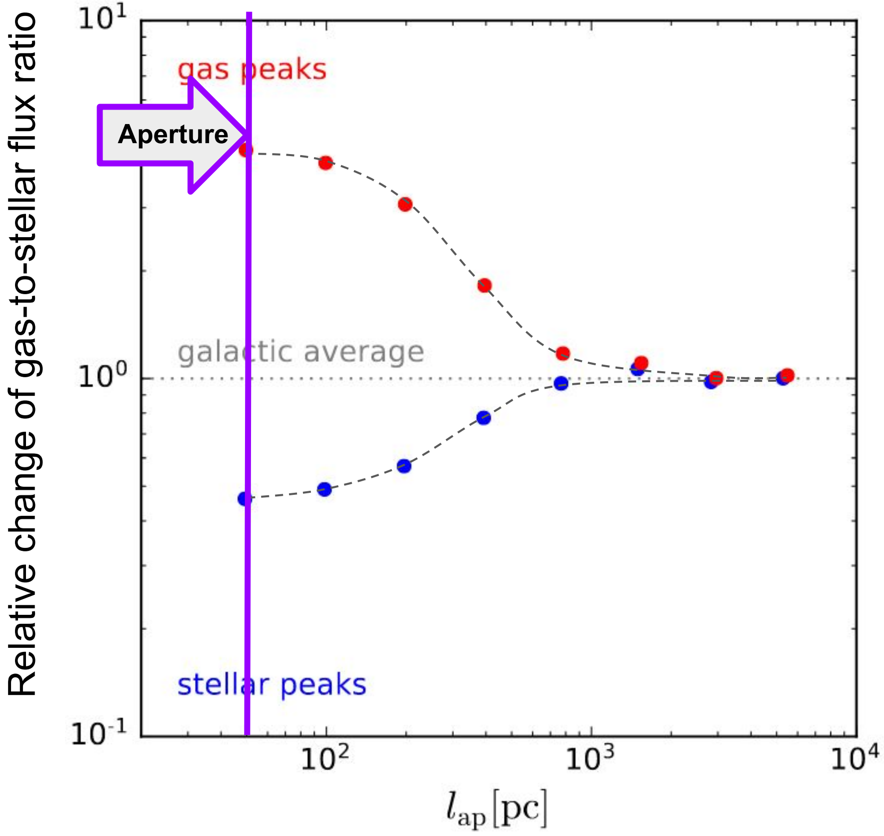

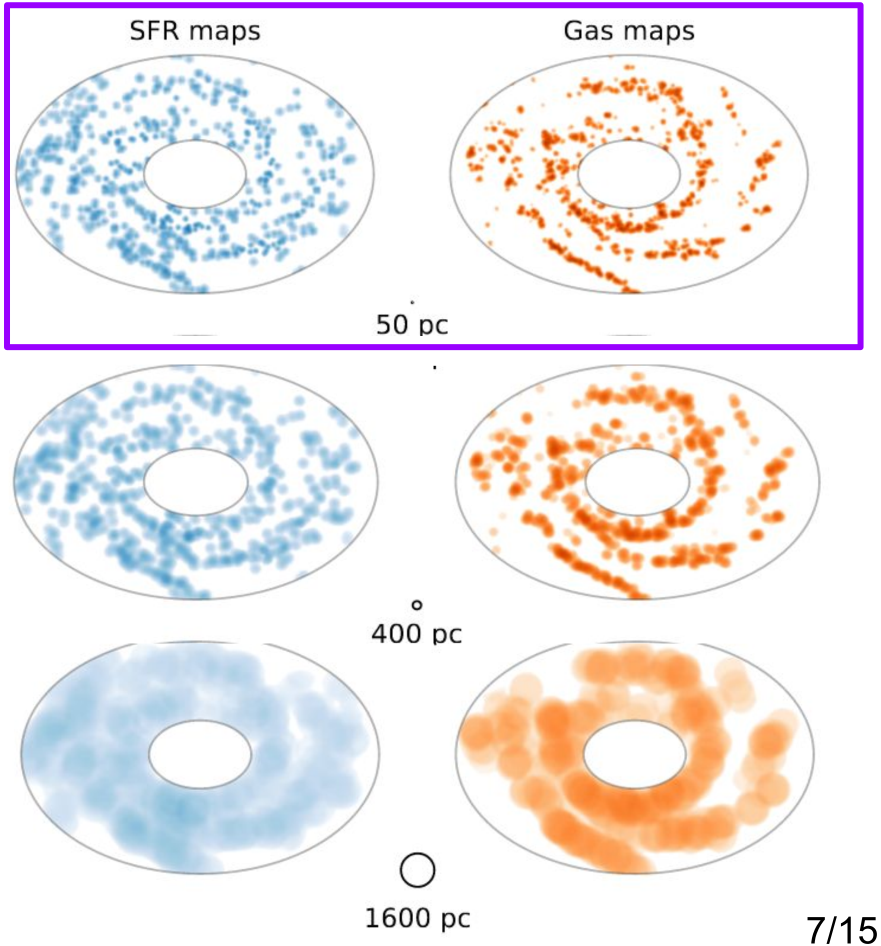

III- 2. The tuning-fork method: exploiting spatial correlations between stars and gas

Kruijssen & Longmore+14
Kruijssen et al. 2018

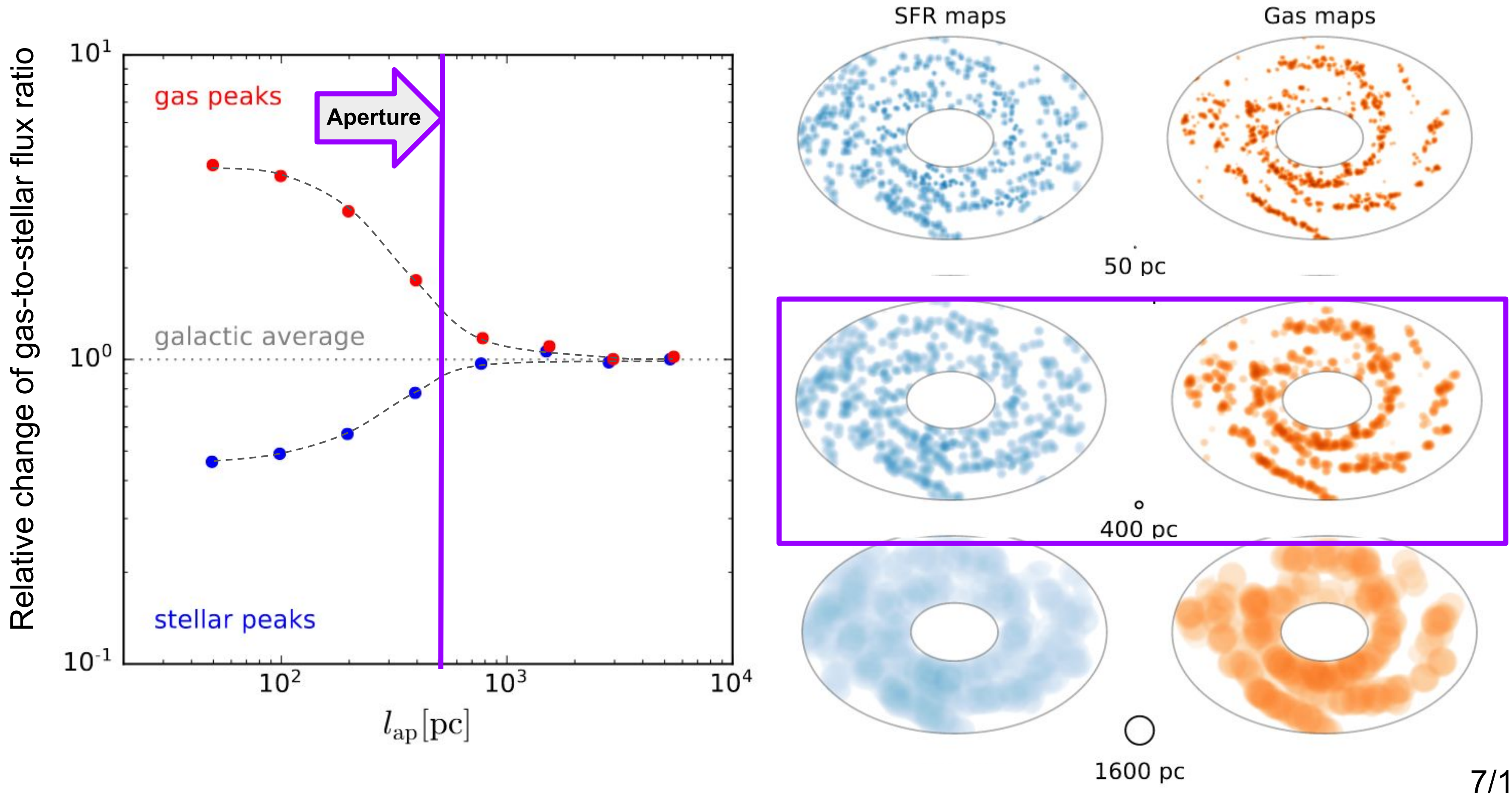

III- 2. The tuning-fork method: exploiting spatial correlations between stars and gas

Kruijssen & Longmore+14
Kruijssen et al. 2018

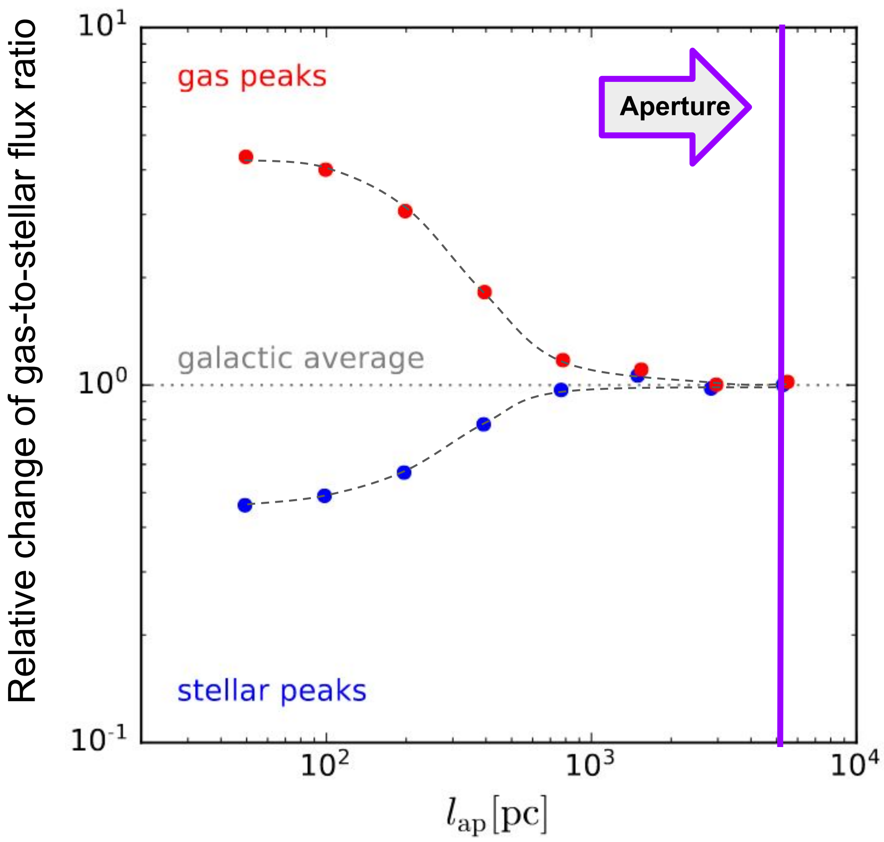

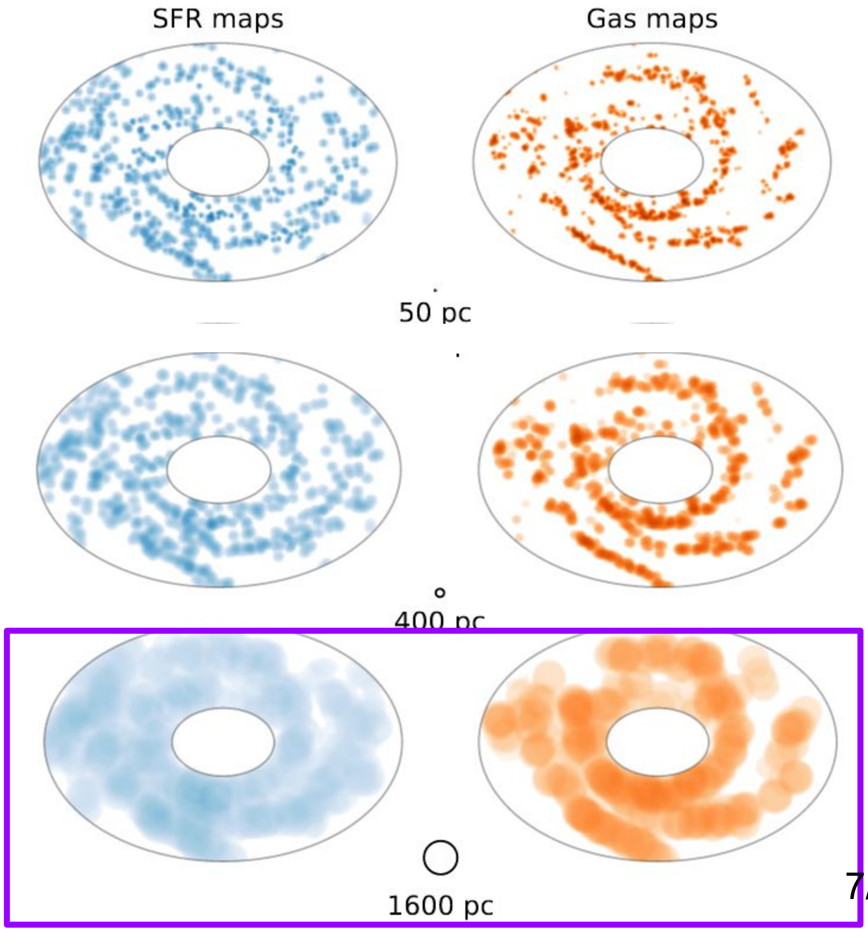

Reproducing gas/star de-correlation in simulations

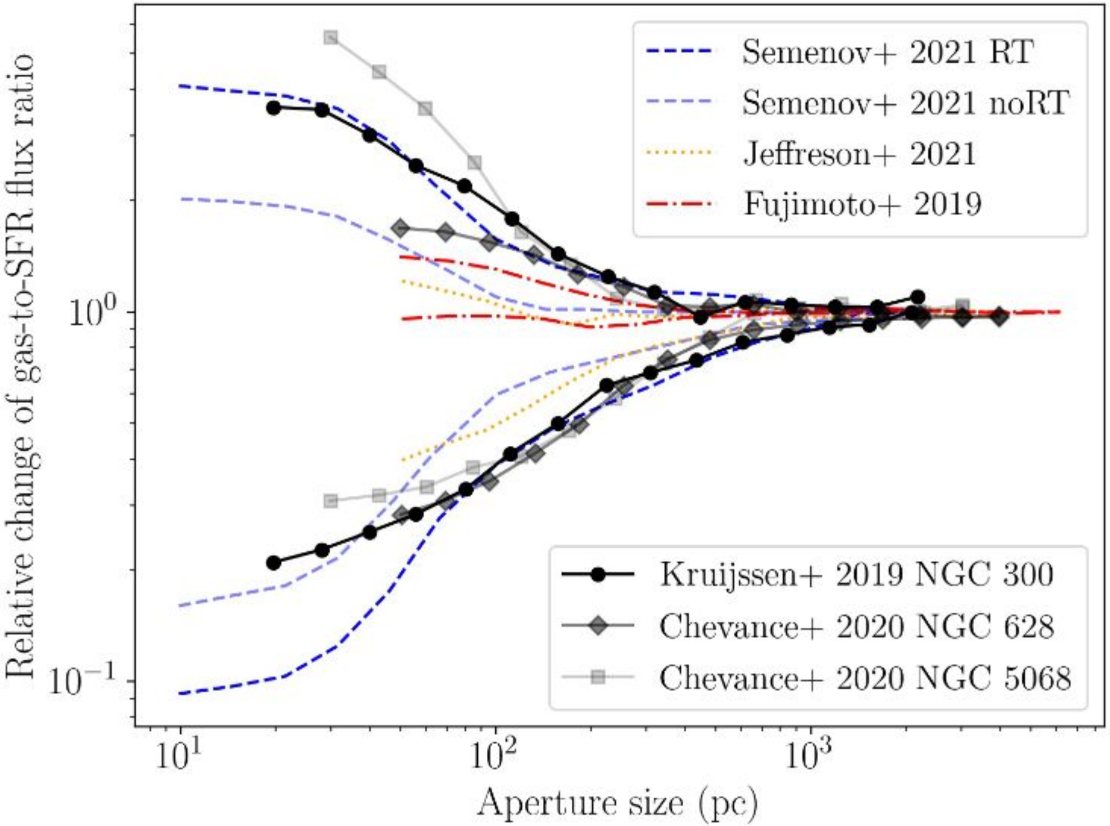

Chevance et al. 2023, PPVII review

Morphological T type (Paturel+98)

range of t	typ	range of typ	type
$-5 \leq t < -3.5$	E	$3.5 \leq t < 4.5$	Sbc
$-3.5 \leq t < -2.5$	E-SO	$4.5 \leq t < 6.5$	Sc
$-2.5 \leq t < -1.5$	SO	$6.5 \leq t < 7.5$	Scd
$-1.5 \leq t < 0.5$	SOa	$7.5 \leq t < 8.5$	Sd
$0.5 \leq t < 1.5$	Sa	$8.5 \leq t < 9.5$	Sm
$1.5 \leq t < 2.5$	Sab	$9.5 \leq t < 10$	Irr
$2.5 \leq t < 3.5$	Sb		

Table 3. Output morphological type codes

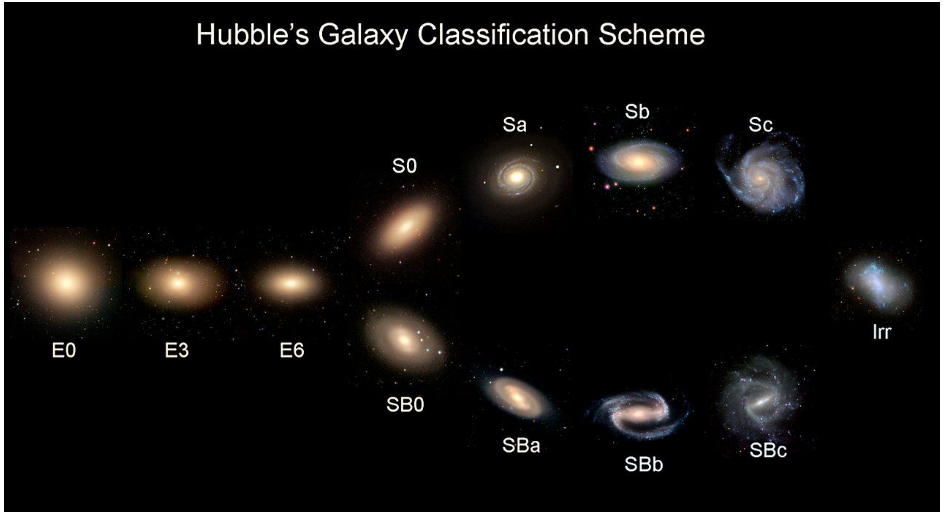

Smaller decorellation scale when using 21um vs Ha as SFR tracer

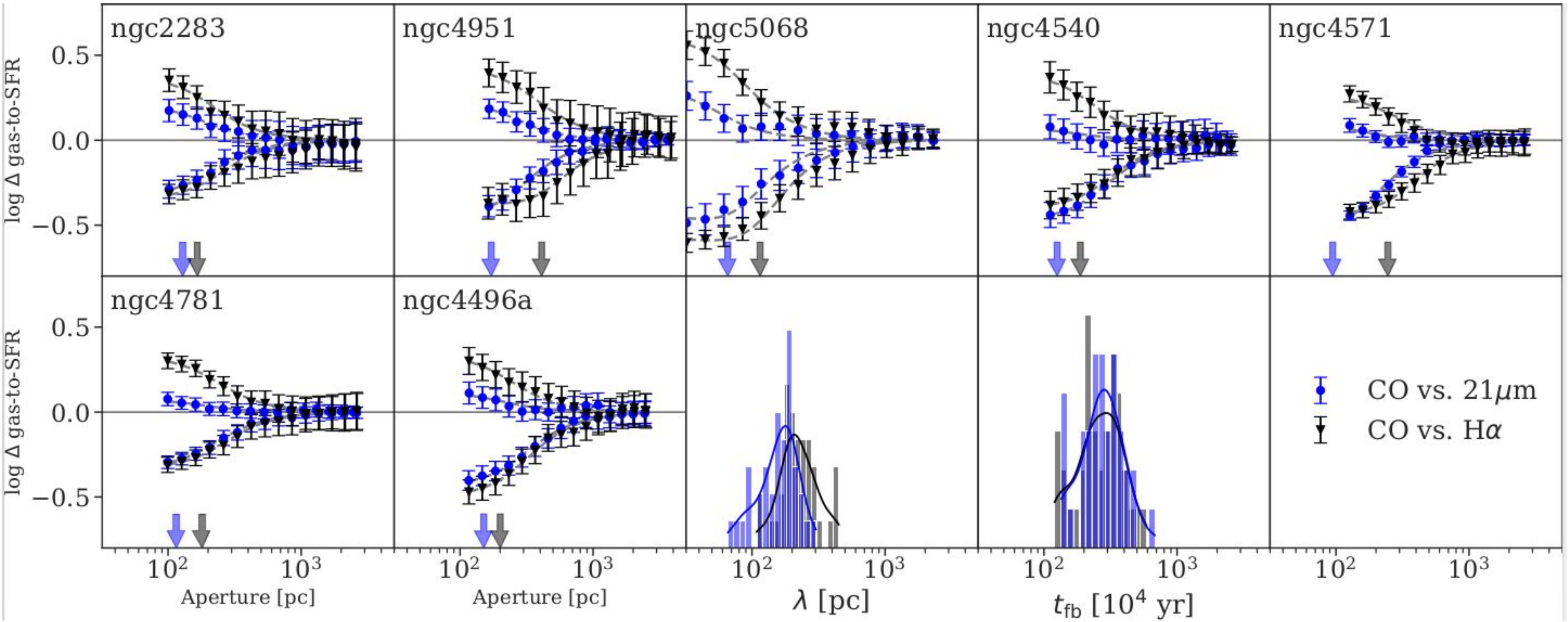

Correlations using the Holm-Bonferroni method

$$p_{\rm eff} = \frac{p_{\rm ref}}{N_{\rm corr} + 1 - i}$$

Global parameters

	M_*	$M_{\rm HI,\,global}$	Δ MS	Hubble type	$M_{\rm gas,\,global}$	$M_{\rm tot,\,global}$	$f_{\rm H_2,\,global}$	$f_{\rm gas,\,global}$	sSFR
$t_{21\mu m}$	**0.42 (-2.02)**	0.38 (-1.66)	0.23 (-0.78)	**-0.46 (-2.36)**	**0.43 (-2.07)**	**0.43 (-2.08)**	0.12 (-0.31)	-0.07 (-0.17)	0.06 (-0.15)
$t_{21\mu m}/t_{\rm CO}$	0.21 (-0.68)	0.39 (-1.78)	0.07 (-0.17)	-0.29 (-1.09)	0.33 (-1.34)	0.24 (-0.82)	-0.2 (-0.63)	0.1 (-0.24)	0.03 (-0.08)
$f^{21\mu m}_{\rm diffuse}$	0.4 (-1.83)	-0.2 (-0.64)	-0.11 (-0.28)	-0.33 (-1.31)	-0.03 (-0.06)	0.35 (-1.49)	**0.52 (-3.0)**	**-0.51 (-2.89)**	-0.3 (-1.13)
$\lambda_{\rm fb,\,21\mu m}$	0.55 (-1.18)	0.57 (-1.29)	0.15 (-0.19)	-0.48 (-0.94)	0.63 (-1.55)	0.53 (-1.12)	0.16 (-0.21)	-0.19 (-0.25)	-0.08 (-0.1)
$t_{\rm fb,\,21\mu m}$	0.64 (-1.62)	0.17 (-0.22)	0.34 (-0.56)	**-0.71 (-2.02)**	0.36 (-0.59)	0.59 (-1.35)	**0.71 (-2.04)**	-0.62 (-1.48)	0.01 (-0.01)
$t_{\rm obscured}$	**0.83 (-3.1)**	0.3 (-0.47)	0.13 (-0.16)	-0.67 (-1.78)	0.57 (-1.29)	**0.8 (-2.79)**	0.68 (-1.81)	**-0.77 (-2.46)**	-0.3 (-0.47)

kpc-scale

	$\Sigma^{\rm kpc}_{\rm SFR}$	$\Sigma^{\rm kpc}_{\rm HI}$	$\Sigma^{\rm kpc}_{*}$	$\Sigma^{\rm kpc}_{\rm H_2}$	$\rho^{\rm kpc}_{*}$	$P^{\rm kpc}_{\rm DE}$
$t_{21\mu m}$	-0.03 (-0.07)	-0.26 (-0.63)	0.13 (-0.35)	0.01 (-0.02)	-0.31 (-1.18)	-0.08 (-0.2)
$t_{21\mu m}/t_{\rm CO}$	-0.13 (-0.35)	0.0 (0.0)	0.06 (-0.14)	-0.26 (-0.92)	-0.29 (-1.09)	0.06 (-0.14)
$f^{21\mu m}_{\rm diffuse}$	0.04 (-0.09)	-0.06 (-0.1)	**0.5 (-2.78)**	0.36 (-1.52)	0.36 (-1.57)	0.05 (-0.12)
$\lambda_{\rm fb,\,21\mu m}$	0.0 (0.0)	**-0.93 (-2.6)**	0.39 (-0.68)	0.12 (-0.15)	-0.29 (-0.45)	-0.59 (-1.38)
$t_{\rm fb,\,21\mu m}$	-0.0 (-0.0)	-0.61 (-0.83)	**0.77 (-2.46)**	0.51 (-1.05)	0.21 (-0.3)	-0.42 (-0.76)
$t_{\rm obscured}$	-0.14 (-0.17)	-0.18 (-0.15)	**0.8 (-2.72)**	0.59 (-1.38)	0.19 (-0.25)	-0.08 (-0.09)

GMC-scale

	$\sigma_{\rm v,\,GMC}$	$\alpha_{\rm vir,\,GMC}$	$M_{\rm GMC}$	$P_{\rm int}$	$\Sigma_{\rm H2,\,GMC}$
$t_{21\mu m}$	**0.54 (-3.24)**	-0.09 (-0.21)	**0.55 (-3.38)**	0.36 (-1.57)	0.28 (-1.01)
$t_{21\mu m}/t_{\rm CO}$	0.35 (-1.47)	0.04 (-0.09)	0.25 (-0.89)	0.23 (-0.76)	0.11 (-0.29)
$f^{21\mu m}_{\rm diffuse}$	**0.44 (-2.19)**	0.01 (-0.01)	**0.44 (-2.21)**	0.4 (-1.83)	0.31 (-1.19)
$\lambda_{\rm fb,\,21\mu m}$	0.58 (-1.32)	-0.31 (-0.48)	0.63 (-1.55)	0.25 (-0.37)	0.24 (-0.35)
$t_{\rm fb,\,21\mu m}$	**0.91 (-4.38)**	-0.35 (-0.58)	**0.92 (-4.55)**	0.67 (-1.77)	0.68 (-1.81)
$t_{\rm obscured}$	0.57 (-1.29)	-0.49 (-0.97)	0.66 (-1.73)	0.62 (-1.48)	0.7 (-1.94)

HII region

	E(B-V)	12+log(O/H)	$L_{\rm mix,\,50\%}$
$t_{21\mu m}$	0.08 (-0.1)	0.54 (-1.87)	0.43 (-0.95)
$t_{21\mu m}/t_{\rm CO}$	-0.18 (-0.29)	0.13 (-0.23)	0.39 (-0.83)
$f^{21\mu m}_{\rm diffuse}$	0.58 (-1.62)	0.48 (-1.47)	0.1 (-0.14)
$\lambda_{\rm fb,\,21\mu m}$	0.4 (-0.54)	0.48 (-0.8)	**0.97 (-4.67)**
$t_{\rm fb,\,21\mu m}$	0.65 (-1.24)	**0.77 (-2.05)**	0.63 (-1.17)
$t_{\rm obscured}$	0.6 (-1.06)	**0.89 (-3.21)**	0.42 (-0.58)

Heisenberg

	$\Sigma_{\rm H_2,\,compact}$	$\Sigma_{\rm SFR}$	M_{H_2}	SFR	$\varepsilon_{\rm CO}$	$\varepsilon_{21\mu m}$
$t_{21\mu m}$	-0.3 (-1.17)	-0.16 (-0.47)	0.07 (-0.17)	0.25 (-0.86)	0.08 (-0.2)	**0.52 (-3.05)**
$t_{21\mu m}/t_{\rm CO}$	**-0.51 (-2.87)**	-0.36 (-1.56)	-0.14 (-0.37)	0.03 (-0.06)	0.15 (-0.41)	**0.55 (-3.33)**
$f^{21\mu m}_{\rm diffuse}$	0.13 (-0.35)	-0.04 (-0.1)	0.14 (-0.39)	0.04 (-0.1)	0.1 (-0.24)	-0.26 (-0.89)
$\lambda_{\rm fb,\,21\mu m}$	-0.04 (-0.05)	-0.35 (-0.58)	0.52 (-1.1)	0.48 (-0.95)	-0.22 (-0.31)	0.06 (-0.06)
$t_{\rm fb,\,21\mu m}$	0.13 (-0.17)	-0.1 (-0.12)	0.35 (-0.58)	0.45 (-0.86)	-0.08 (-0.1)	0.1 (-0.12)
$t_{\rm obscured}$	0.15 (-0.2)	-0.1 (-0.12)	0.46 (-0.88)	0.47 (-0.9)	0.13 (-0.16)	0.51 (-1.05)

Systematics

	$l_{\rm ap,\,min}$	i	c
$t_{21\mu m}$	0.26 (-0.91)	-0.02 (-0.05)	0.01 (-0.01)
$t_{21\mu m}/t_{\rm CO}$	0.18 (-0.55)	0.14 (-0.39)	-0.19 (-0.6)
$f^{21\mu m}_{\rm diffuse}$	0.3 (-1.15)	0.11 (-0.28)	0.19 (-0.58)
$\lambda_{\rm fb,\,21\mu m}$	**0.8 (-2.72)**	0.38 (-0.66)	0.42 (-0.76)
$t_{\rm fb,\,21\mu m}$	0.53 (-1.12)	0.52 (-1.1)	0.43 (-0.8)
$t_{\rm obscured}$	0.03 (-0.04)	0.29 (-0.44)	-0.04 (-0.05)

III - Results : measuring the timescales associated with the dust-embedded SF

2. Which parameters regulate the duration of the dust emission at 21um ?

Ramambason et al. in prep

Total duration of 21µm emission

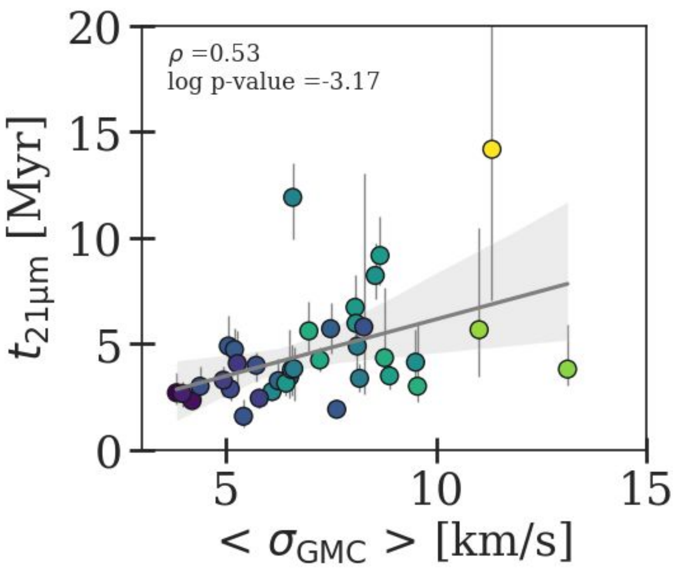

Duration of the feedback phase

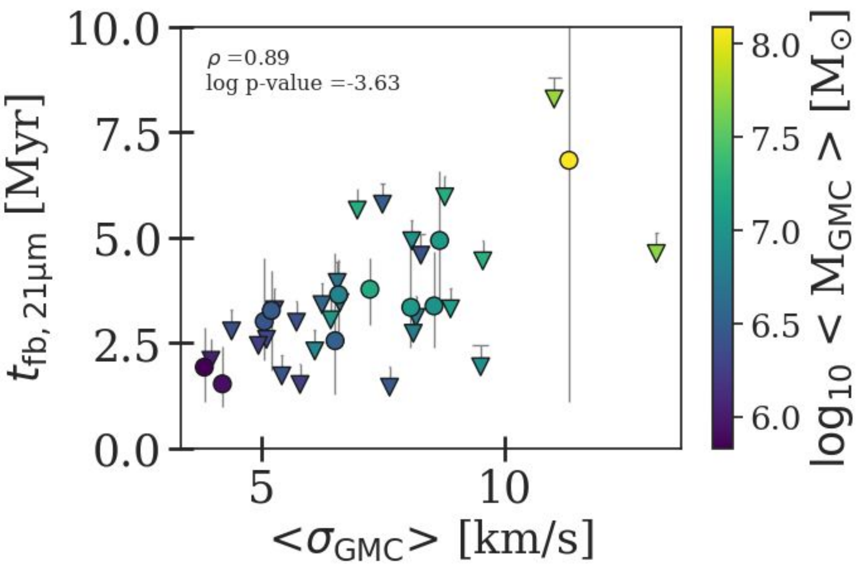

⇒ **Increased duration** of the 21µm emission and feedback phase in galaxies with :

- more **massive GMCs**
- higher **velocity dispersion**

Additional correlations

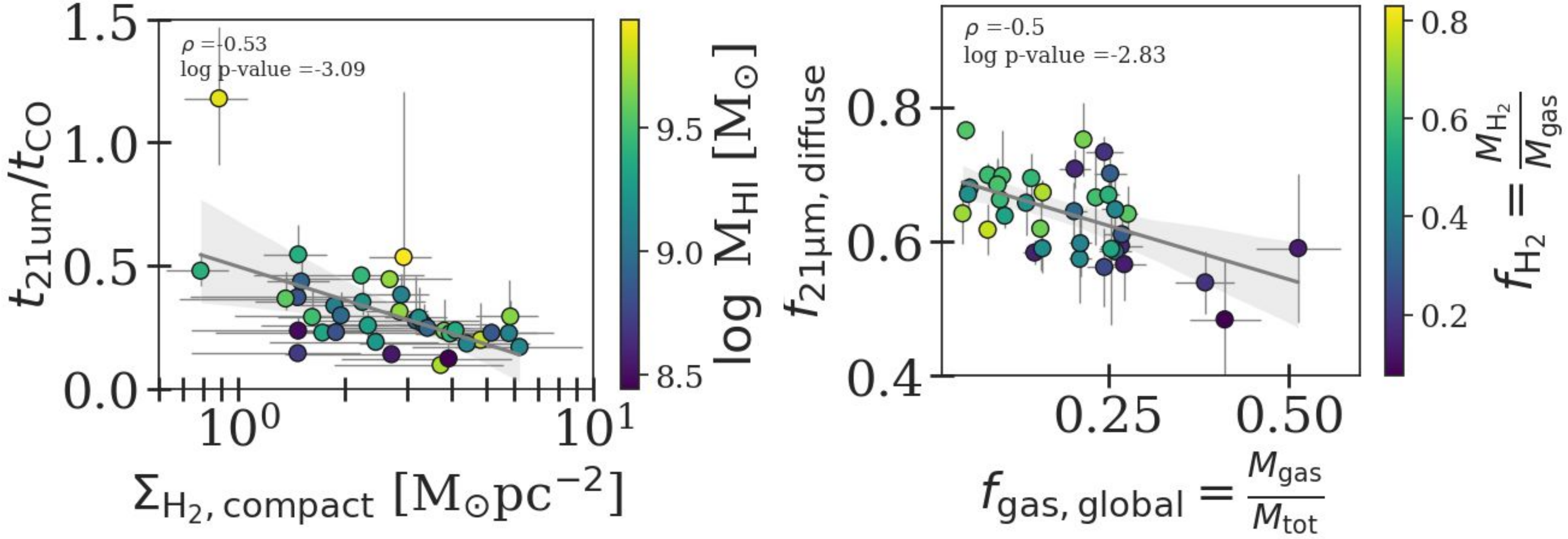

III - 3. Results : measuring the timescales associated with the dust-embedded SF

2. Which parameters regulate the timescales of the dust emission at 21um ?

Ramambason et al. subm

Star/GMC coupling efficiency (*Chevance+20a*)

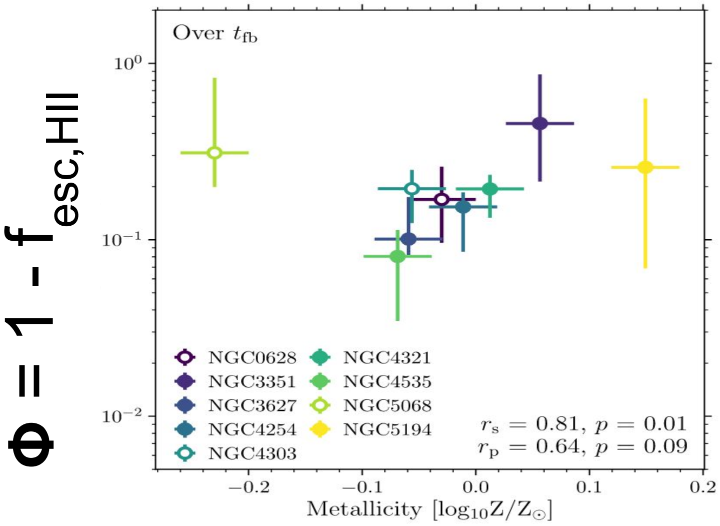

Duration of the obscured SF phase

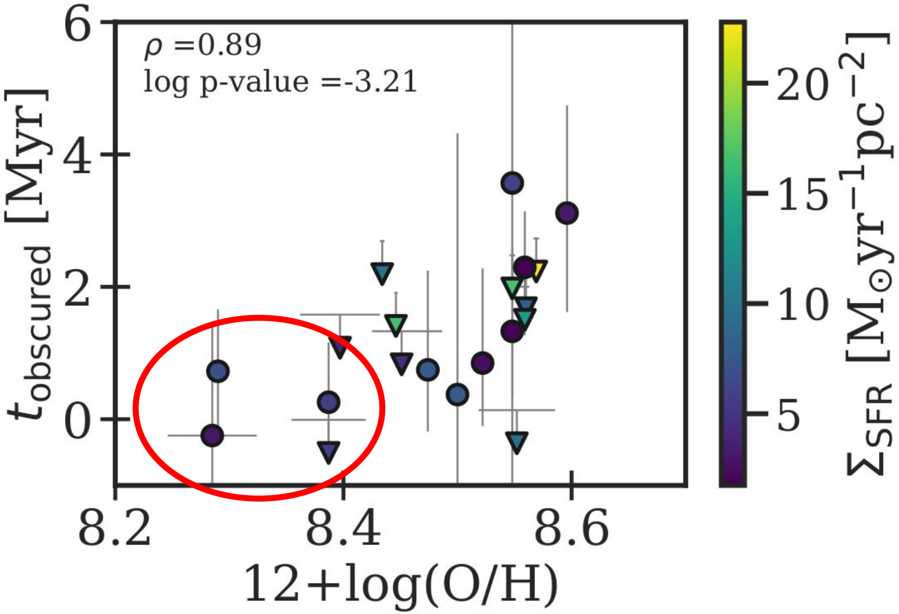

⇒ increased duration of the 21µm emission and duration obscured SF phase in galaxies with <u>higher metallicity ?</u> → **effect of increased ISM porosity at low-Z?**

observed at galactic scales e.g., Cormier19, Chevance+20b, Ramambason+22,+24

II- 3. Application of MULTIGRIS: escape fractions of ionizing photons *(Ramambason+22)*

- **model = combination of** 1,2 or 3 components (Cloudy)

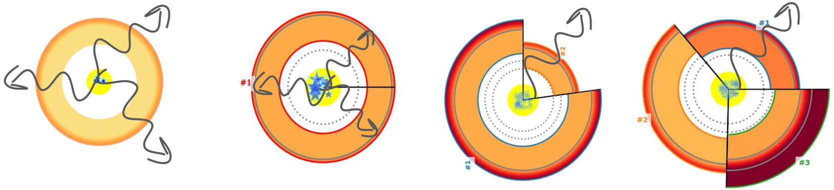

- data = suite of IR lines tracing the ionized and neutral atomic gas

Neutral and ionized gas tracers	[O I]λλ63,145μm [Fe II]λλ17,25μm (7.9eV), [Si II]λ34μm (8.2eV), [C II]λ158μm (11.3eV), Huαλ12μm (13.6eV), [N II]λλ122,205μm (14.5eV), [Ar II]λ7μm (15.7eV), [Fe III]λ23μm (16.2eV), [Ne II]λ12μm (21.6eV), [S III]λλ18,33μm (23.3eV), [Ar III]λλ9,21μm (27.6eV), [N III]λ57μm (29.6eV), [S IV]λ10μm (34.7eV), [O III]λ88μm (35.1eV), [Ne III]λ15μm (40.9eV) [O IV]λ26μm (54.9eV), [Ne V]λλ14,24μm (97.1eV),
Total infrared luminosity	$L_{\rm TIR}$ (1μm-1000μm)

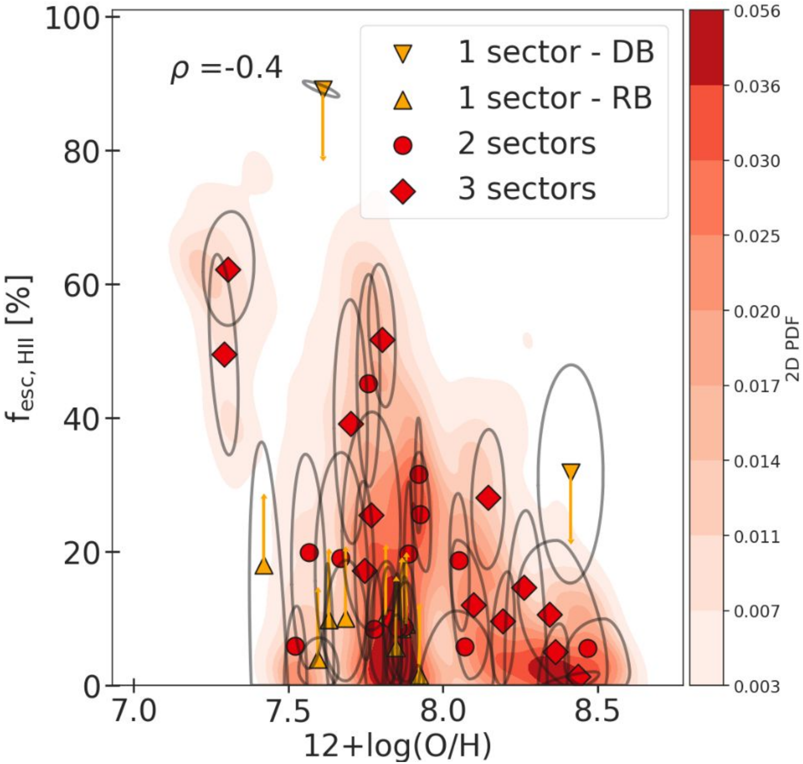

Main result with multicomponent models:
Relatively high predicted escape fractions of ionizing photons, decreasing metallicity and increasing sSFR.